

# Modeling lightning-NO<sub>x</sub> chemistry at sub-grid scale in a global chemical transport model

A. Gressent<sup>1</sup>, B. Sauvage<sup>1</sup>, D. Cariolle<sup>2, 3</sup>, M. Evans<sup>4, 5</sup>, M. Leriche<sup>1</sup>, C. Mari<sup>1</sup>, and V. Thouret<sup>1</sup>

1: LA, CNRS, Université Paul Sabatier III de Toulouse, Toulouse, France

2: Météo France, Toulouse, France

3: Centre Européen de Recherche et de Formation Avancée en Calcul Scientifique, CERFACS, Toulouse, France

4: Wolfson Atmospheric Chemistry Laboratories (WACL), Department of Chemistry, University of York, York, YO10 5DD, UK

5: National Centre for Atmospheric Science (NCAS), University of York, York, YO10 5DD, UK

---

The authors thank the referees for their comments on the manuscript. Their suggestions of correction and their questions on this work are very interesting and definitely help to improve this paper.

## Referee #1:

### Specific comments:

- \* *P34100 L8-11: Is there a reason that the methods used to determine horizontal dispersion could not be used to find vertical dispersion as well? A greater understanding of vertical dispersion could be used to augment the profiles used to force the vertical distribution of LNO<sub>x</sub> given by Ott et al. If this is beyond the scope of this study as the authors indicate, that is fine, and a sentence or two explaining why would suffice. Also, is the claim that vertical diffusion is less efficient than horizontal diffusion really true for the strong convective storms that create lightning?*

We thank the referee#1 for his useful comment on the atmospheric diffusion issue. We agree that lightning triggering and NO<sub>x</sub> emissions from electrical discharges occur in the convective part of the cloud where the vertical diffusion (D<sub>v</sub>) is stronger than the horizontal diffusion (D<sub>h</sub>). Therefore, the vertical diffusion coefficient is a determining parameter for the LNO<sub>x</sub> distribution. However, this vertical distribution of LNO<sub>x</sub> is a priori estimated from Ott et al., 2010, as a reverse “C-shape” profile, prescribed in GEOS-Chem, and totally independent of our parameterization. It could be very interesting to estimate D<sub>v</sub> in the cloud to improve and support the Ott et al., 2010 given LNO<sub>x</sub> vertical profile using similar methods than the one used in the present study. This is indeed beyond the scope of our study, as it would require taking over Ott et al., 2010 work. Moreover, the plume parameterization for LNO<sub>x</sub> chemistry is applied a posteriori after lightning NO<sub>x</sub> are vertically prescribed by Ott et al., 2010 and emitted in convective clouds. Our parameterization starts just after transport driven by the convective parameterization and will then mostly concerns convective outflow where the NO<sub>x</sub> are detrained in the troposphere. In this region of detrainment, the horizontal diffusion seems to be more efficient than the vertical one as mentioned by Cariolle et al., 2009. Also, future studies on the atmospheric diffusion such as in-situ measurements and meso-scale modeling calculations should be useful to better quantify D<sub>v</sub> and D<sub>h</sub>.

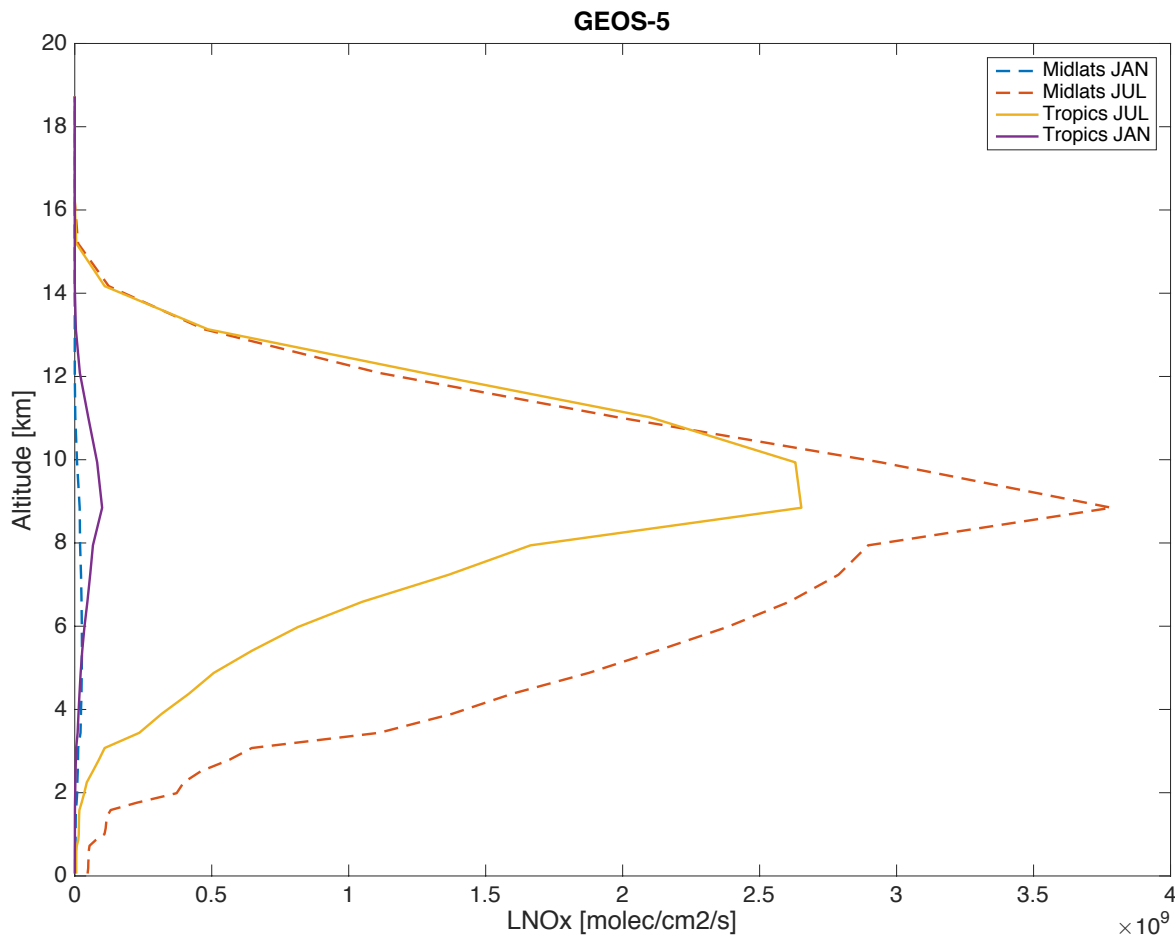
According to this explanation we have clarified this point in the text, section 3.1.1 as follows: “Note that the mean dispersion properties of the atmosphere were associated with the horizontal diffusion only. The lightning NO<sub>x</sub> emissions occur in the convective part of clouds where the vertical diffusion is strong. Therefore, the vertical diffusion coefficient is a determining parameter for the LNO<sub>x</sub> distribution in the cloud. As mentioned in section 2.1, the vertical distribution of the LNO<sub>x</sub> is a priori calculated from Ott et al. (2010) as a reverse C-shaped profile. The LNO<sub>x</sub> plume parameterization is applied a posteriori after that lightning NO<sub>x</sub> are vertically prescribed and concerns convective outflow where the NO<sub>x</sub> are detrained in the troposphere. In this region of detrainment, the horizontal dispersion may be more efficient than the vertical one as discussed in Cariolle et al., 2009. “

- \* *P34109 L8: I wonder about choosing the 8-11 km range. A brief explanation as to why this range was chosen would be appreciated. Is it appropriate to use the same vertical range for tropical and midlatitude storms, given the differences in their convective depth? How will this affect the parameterization of lightning outside of this range (or, how sensitive are the results to altitude)?*

Referee comment is legitimate. In a real atmosphere the detrainment region is commonly observed at higher altitude (up to 13-14km altitude, Folkins and Martin 2004, doi: <http://dx.doi.org/10.1175/JAS3407.1>) in the tropics than in the mid-latitudes (8-9 km altitude, DeCaria et al. 2000) In this study, the GEOS-Chem model uses GEOS-5 meteorological fields. The following figure illustrates the vertical distribution of the LNO<sub>x</sub> calculated by GEOS-Chem with GEOS-5 for the tropics and the mid-latitudes. This figure shows that the detrainment altitude is similar in both regions, i.e. around 8-11 km. GEOS-5 seems to underestimate the detrainment altitude in the tropics as shown in a previous work (Folkins et al., 2006, doi:10.1029/2006JD007325). Therefore, we decided to show vertical levels consistent with the GEOS-5 detrainment altitude level.

Outside this altitude range, our parameterization should mainly have influence between 6 and 12 km for which the calculated LNO<sub>x</sub> flux is still significant both in the tropics and in the mid-latitudes as showed by the following figure. However, the impact should be less important than between 8-10 km where the LNO<sub>x</sub> flux is the strongest.

We clarified this point in the manuscript, section 3.2.2 as follows: “The altitude range refers to the detrainment region estimated by GEOS-Chem using the GEOS-5 met fields (section 2.1) both in the tropics and in the mid-latitudes. Note that this range could vary depending on the met fields and the convection parameterization. In addition, the LNO<sub>x</sub> plume parameterization might have an impact outside of this altitude range mainly between 6 km and 12 km but in a lesser extent”.



\* P34108 L16-: The authors indicate that 3-D turbulence is solved in their parameterization, and give a range of  $D_h$  values. More discussion of this would be interesting. How does  $D_h$  vary globally? Are there any trends or features in the  $D_h$  fields that are of interest? I, and I imagine other readers as well, would be interested in more details on the variability.

The 3-D turbulence is actually not solved online in the GEOS-Chem CTM because of the fine scale characterizing this process but prescribed by the met fields (GEOS-5). Therefore, the global variability of  $D_h$  is not calculated in the model and has to be deduced a priori. For our parameterization, in order to determine  $D_h$  in the outflow region (i.e. at small scale), we have used both meso-scale modeling and in-situ measurements in the cloud anvil. The three-estimated  $D_h$  values [0.1; 15; 100] m<sup>2</sup>.s<sup>-1</sup> are very dispersed. There is a real gap to fill about the knowledge in this parameter in the upper troposphere and especially in the outflow region. In the future, further meso-scale modeling studies and in-situ measurements in the scientific community should help to better define  $D_h$  variability.

We clarified this point in the revised version of the paper, section 3.2.1 as follows: “It is important to note that the 3-D turbulence is not solved online in the GEOS-Chem model because of the fine scale characterizing this process but prescribed by the GEOS-5 met fields. Therefore, the global variability of  $D_h$  is not calculated by the CTM and it is beyond the scope of this study.”.

- \* *P34110 L25-: The ratio  $R_{\text{LNOx}}$  is set to be consistent with GEOS-Chem. It's good to be consistent, but I wonder if more can be said regarding this issue since this is a problem that is poorly understood. Is there anything in the parameters used in the new plume-in-grid parameterization that can shed some insight into what drives this difference between midlatitudes and tropics? This is related to my previous comment regarding variability of  $D_h$ . More discussion on the spatial variability of the various model parameters may be enlightening.*

As the referee pointed out, there are large differences in the LNOx production between the tropics and the mid-latitudes. The rate of flashes is higher in the tropics (Christian et al., 2003) but the amount of NOx molecules emitted per flash might be higher in the mid-latitudes. The amount of NOx molecules produced per flash may depend on different lightning parameters such as the number of flashes, but also the flash length, the stroke peak current and the stroke release height (Huntrieser, 2008, <http://www.atmos-chem-phys.net/8/921/2008/acp-8-921-2008.pdf>).

Our study aims to improve and represent the chemistry related to lightning NOx emissions in CTMs at global scale. The approach applied here is the implementation of a parameterization, which includes uncertainties regarding parameters estimate. The main parameters defined in this study could help us to get a more realistic idea of the NOx then O3 distribution at global scale. Also, the variability of these parameters may depend on latitude, as it is mainly the case for the plume lifetime. The horizontal diffusion coefficient doesn't appear directly in the plume parameterization in the CTM. It is estimated beforehand and used in the simple plume dispersion simulations. Therefore, we don't use and show the horizontal diffusion at global scale and the related variability.

The suggestion of the referee to use our results for understanding the tropics and the mid-latitudes LNOx emissions differences is interesting. However this is not easily feasible as our parameterization is linked with the convective and LNOx emission parameterizations used in the CTM, for which dependence on the tropics and mid-latitudes differences in terms of convective intensity and LNOx emissions are already considered (GEOS-Chem model, [http://wiki.seas.harvard.edu/geos-chem/index.php/Lightning\\_NOx\\_emissions](http://wiki.seas.harvard.edu/geos-chem/index.php/Lightning_NOx_emissions)). Using similar LNOx emissions in the CTM (no a priori latitude dependence,  $RLNOx=1$ ) with our sub-grid scales parameterizations, validated with in situ LNOx measurements, should indeed better help understand the  $RLNOx$  ratio, as suggested by referee#1. However, it would certainly require more LNOx observations in the tropics, poorly documented, as already stated in the manuscript.

- \* *Section 4.2: The comparisons between different model simulations (BC, P1, P2 experiments) do not include a direct comparison between the full model with and without the plume parameterization. Section 4.2.2 effectively does this by using the difference between P1 and BC experiments, but I found this to be unnecessarily confusing. A separately named direct comparison would be clearer to the reader.*

As suggested, we have changed the (P1-BC) difference by a direct comparison name (P3) in order to make the comparison clearer to the reader.

- \* P34115 L5-6 “an approximate detrainment level (9 km altitude) where the LNO<sub>x</sub> are most concentrated”: This sentence is a bit unclear. Is this the level where most LNO<sub>x</sub> is produced, or the level where the detrainment of LNO<sub>x</sub> from a cloud is the largest?

We thank the referee#1 for this good remark. Regarding the results in the entire vertical, the 9 km level corresponds to the altitude where the detrainment level of LNO<sub>x</sub> is the largest.

We have clarified this point in the text in section 4.2.1 as follows: “These results are shown for an approximate detrainment level (9km altitude) where the detrainment of LNO<sub>x</sub> is the largest.”

- \* Section 4.2.1: The differences in plume lifetime for different seasons and locations are given without context. What drives these differences?

The plume lifetime ( $\tau$ ) depends directly on, first, the NO<sub>x</sub> content ( $rl$ ) above which the LNO<sub>x</sub> plume exists. This critical value changes mainly with the latitude since its calculation is initialized by the background concentrations of species, which are different in the tropics and in the mid-latitudes regions (see Table 1). Then,  $\tau$  varies depending on the amount of LNO<sub>x</sub> emitted by lightning (NO<sub>i</sub> in the manuscript), which is higher in the tropics than in the mid-latitudes as mentioned previously. We do not show seasonal variations of  $\tau$  (because they are negligible). However, day and night conditions strongly influence the  $rl$  calculation. Therefore, we calculate different values of  $\tau$  for daytime and nighttime (Table 2). The seasonal variations are presented only for NO<sub>y</sub> and O<sub>3</sub> distributions at global scale.

As suggested by the referee we clarified this point in the manuscript, section 4.2.1 as follows: “The plume lifetime depends on the latitude because of the different background chemical concentrations and the different amount of NO<sub>x</sub> emitted from lightning in the tropics and in the mid-latitudes. In addition, as mentioned before, we consider the influence of day and night conditions on the plume lifetime estimate.”.

- \* P34115 L27: Why are some emissions “less important”? Does this just mean there are fewer emissions, or is something making them less important somehow?

We agree with the referee that the expression “less important” is unclear to qualify the lightning NO<sub>x</sub> emissions. We mean fewer emissions and we have changed the sentence in the text, section 4.2.1, as follows: “So, the LNO<sub>x</sub> tracer is characterized by a shorter lifetime as a plume over North America than over Central Africa and around the Sahel while the model simulated fewer emissions over these regions especially in summer.”

- \* P34116 L5: what do you mean by “tracer is mainly reproduced”?

We agree with the referee that this sentence is unclear and we have removed the term “mainly”. Indeed, lightning NO<sub>x</sub> emissions are distributed from the surface to the cloud top height by the CTM according to the reverse “C-Shape” profile (Ott et al., 2010). Results show that the tracer mixing ratio is reproduced at the altitude where lightning emissions are calculated and detrained, mainly in the upper troposphere. This sentence aims to point out the consistency between lightning NO<sub>x</sub> emissions and the tracer distributions.

- \* P34121 L1 *“Significant values of B”: How large does B have to be to be significant? Or does this just mean non-zero?*

We thank the referee#1 for this good comment. Our estimates of the  $\beta_1$  ( $10^{-4}$ ) and  $\beta_2$  ( $10^{-3}$ ) fractions are smaller than those from Cariolle et al., 2009 (with  $\beta_1=0.06$  and  $\beta_2=0.2$ ) in which the effects of the  $\beta$  fractions are non-negligible on the NO<sub>y</sub> distribution. Therefore, we assumed that if the  $\beta$  fractions would be higher than our estimates, their impact should be significant regarding Cariolle et al., 2009 results. Further modeling studies are needed (both box model and CTM) in order to determine what could be the significant values for the  $\beta$  fractions.

- \* Figure 9: *The hatched areas are a bit hard to read since they overlap with multiple lines. The authors may want to consider revising this figure to make it clearer.*

We agree with the referee#1 comment. The figure 9 has been modified to make it clearer.

- \* P34101 L5 *“than the surrounding” should be “as the surrounding”*

This has been changed in the revised version of the manuscript.

- \* P34108 L22 *“cover all of horizontal” should be either “cover all horizontal” or “cover all of the horizontal”*

This has been changed in the revised version of the manuscript.

- \* P34110 L16 L18 *“the northern Colorado” and “the Ontario”. The “the” should be removed.*

This has been changed in the revised version of the manuscript.

- \* P34111 L 24-25: *This sentence is confusing and should probably be re-worded.*

The sentence was re-worded as suggested by the referee#1 as follows: “Our  $K_{\text{eff}}$  estimates are smaller than those calculated by Cariolle et al. (2009) for the plume chemistry related to aircraft exhausts. In this previous work,  $K_{\text{eff}}$  varies from 1.0 to  $4.2 \cdot 10^{-18}$  molecules<sup>-1</sup> s<sup>-1</sup> cm<sup>-3</sup> with a mean value close to  $3 \cdot 10^{-18}$  molecules<sup>-1</sup> s<sup>-1</sup> cm<sup>-3</sup> depending on the NO<sub>x</sub> loading. The very low value for  $K_{\text{eff}}$  point out that the plume parameterization implies a delay of the production of ozone at the large scale rather than its destruction within the plume.”

- \* P34121 L8-11: *The sentence beginning “That could be explained” is also confusing and needs to be re-worded.*

The sentence was re-worded as suggested by the referee#1 as follows: “Indeed, our  $\beta_1$  and  $\beta_2$  estimates are smaller than those calculated by Cariolle et al., 2009 ( $\beta_1 = 0.06$  and  $\beta_2 = 0.2$ ) which showed a significant impact of this mechanism in the case of aircraft NO<sub>x</sub> emissions.”

## Referee #2:

- \* *Lightning emissions are of NO, not NO<sub>x</sub>. It would be helpful if the paper discussed this from the beginning and not waiting until Section 4 to clarify this.*

We agree with the referee#2 comment and we have clarified this point at the beginning of the Introduction as follows: "Lightning emissions are one of the most important sources of nitrogen oxides ( $\text{NO}_x \equiv \text{NO} + \text{NO}_2$ ) in the upper troposphere (WMO, 1999; Hudman et al., 2007). Lightning primarily produce NO and may also induce a negligible quantity of NO<sub>2</sub> with a ratio NO<sub>2</sub>/NO<sub>x</sub> of 0.5 to 0.1 (Franzblau, 25 1991; Stark et al., 1996)."

- \* *p. 34101: the Ox family is O + O<sub>3</sub> + NO<sub>2</sub> (not O<sub>2</sub>!)*

This has been changed in the revised version of the manuscript.

- \* *The English needs to be corrected throughout the paper - there are numerous mismatches of plural-singular, and extraneous or missing articles (the, a). Also, for example, on p. 34106, 'allows to form' should be 'allowing formation of'.*

We thank the referee#2 for his/her comment. We have corrected the English throughout the paper.

### Referee #3:

#### General comments:

1. *The plume parameterization uses both mixing ratios (molecules/molecules; all the variables that start with “r”) and concentrations (molecules/cm<sup>3</sup>) in its equations, so it is important that the text correctly refer to each to avoid confusion. However, the original C09 equations have not had their units correctly translated to this paper. For example, Equation (2) labels  $r_p$  as a concentration (molecules cm<sup>-3</sup>), but it needs to be a mixing ratio in order for its integration with air density ( $\rho$ ) to yield molecules. The subsequent continuity equations, especially the  $d(rO_3)/dt$  equation, are also dependent on a careful distinction of concentration versus mixing ratio in its components. The authors will either need to maintain the original units from C09 in all their equations (a mix of both mixing ratios and concentrations), or reformulate them such that they are all concentrations as they are currently described (e.g., removing  $r$  where necessary, changing  $rO_3$  to  $[O_3]$ , etc.). I also recommend removing the multiplication crosses in the equations, and think it would be easier for the reader if standard square brackets were used for the concentrations in Equations (5)-(7), e.g.,  $d([O]+[O_3])/dt = k_2 [NO_2] - k_3 [NO][O_3] \dots$*

We agree with the suggestion of the referee#3. The related changes have been made in the text for describing the equations with the appropriate terms according to Cariolle et al., 2009.

2. *It is not clear to me what model is being used to estimate  $\tau$  and  $K_{eff}$ , which requires resolving chemistry and transport on spatiotemporal scales finer than the plume itself. I think the model section needs an additional part that describes the “simple plume dispersion” model referenced in Sections 3.2.3 and 3.2.4, in particular how the chemistry was included that was used to determine  $K_{eff}$ .*

We agree with the referee comment. We have added the section 2.4 to the manuscript in order to present the simple plume dispersion model for determining  $\tau$  and  $K_{eff}$  as follows:

“To model the dispersion of lightning NO<sub>x</sub> emissions we use a simple dispersion model similar to the plume model used for aircraft NO<sub>x</sub> emissions, except that the plume is supposed to be oriented along a vertical axis. The plume is represented as a cylinder that encompass horizontal diffusion with a constant coefficient  $D_h$  (section 3.2.1). This simple model is composed of 30 horizontal circles with spacing increasing progressively from the center axis. The discretization of the diffusion equation is mass conservative.

The chemistry scheme and associated reaction rate constants is adapted from the large-scale chemical model MOCAGE (Teyssedre2007). It includes the main reactions involved in the NO<sub>x</sub>-HO<sub>x</sub> system. Simple plume simulations were performed in order to estimate the physical and chemical characteristics of plumes related to lightning NO<sub>x</sub> emissions.”

3. *The formulation of  $K_{eff}$  in C09 assumes that only NO<sub>x</sub> is elevated in the plumes relative to the diluted background mean (whereas other species are assumed to match the background at the initialization of the plume). This is a decent assumption for aircraft and ships, but less so for lightning. Lightning NO<sub>x</sub> is released during active deep convection, by which sub-grid-scale processes rapidly mix air from non-local locations, yielding complex*



*mixtures of ozone, VOC, HOx and H2O observed in convective outflows that would be atypical relative to the background grid cell. For example, the recent DC3 campaign saw complex mixtures of surface and stratospheric air masses alongside lightning NOx plumes (doi:10.1175/BAMS-D-13-00290.1). I think that the authors should briefly acknowledge these uncertainties and how they might affect their conclusions.*

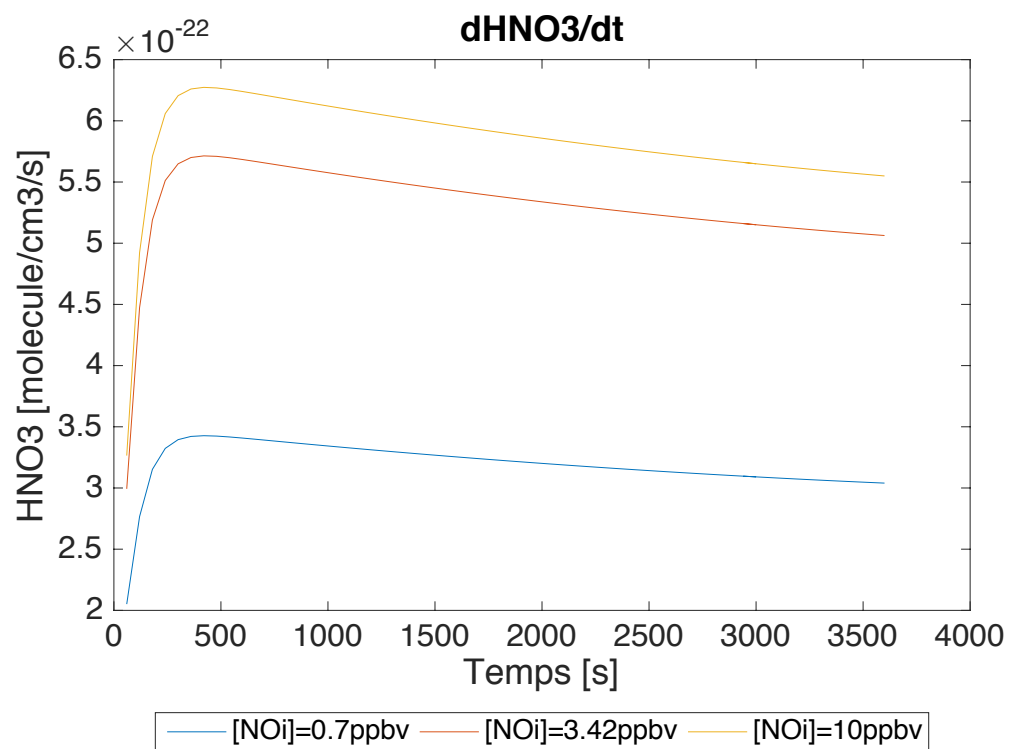
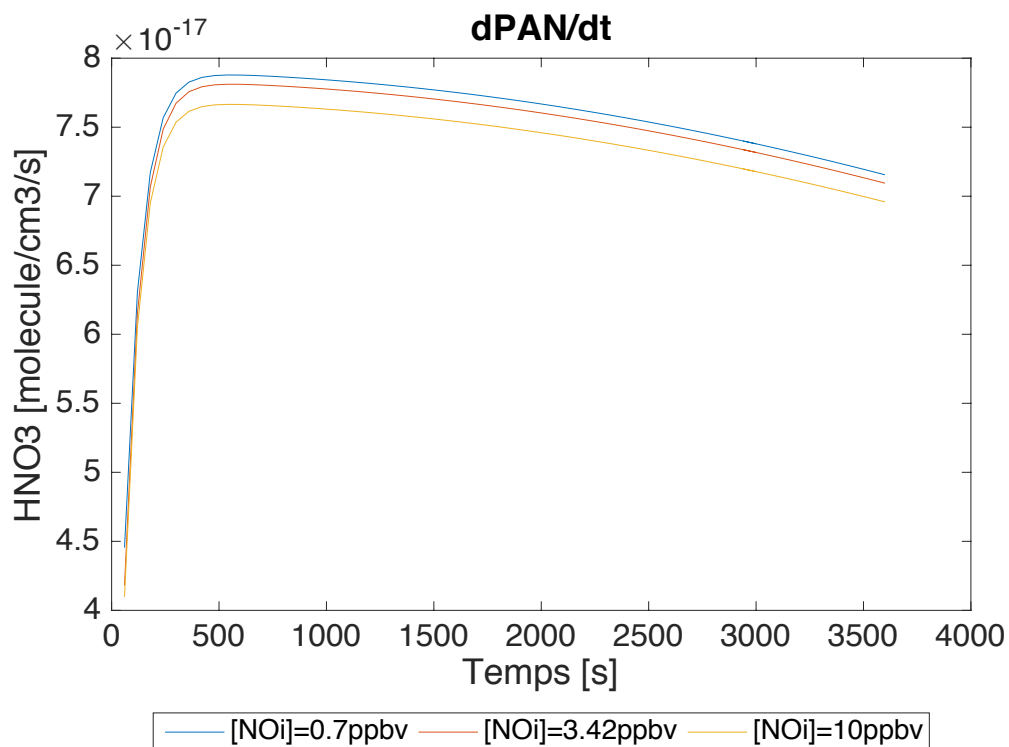
The comment about the  $K_{\text{eff}}$  calculation from the referee#3 is very interesting. We agree that in the case of lightning emissions other species like VOCs, HOx and H2O may be uplifted from the surface in the convective region. Nevertheless, Sauvage et al., 2007 showed that, in the upper troposphere, NOx rather than VOCs mainly influence O3 mixing ratio. In other words, the OPE in the UT is controlled by NOx. We assumed that our plume parameterization is a first estimate of the LNOx chemistry focused on NOx.

As suggested by the referee, we have clarified this point in the manuscript in section 3.2.4 as follows: “Note that in the case of lightning emissions other species like VOCs, HOx and H2O may be uplifted in the convective region that could bring uncertainties in our approach. However, we assumed that the OPE is mainly controlled by NOx in the upper troposphere as previously showed by Sauvage et al. (2007b). Therefore,  $K_{\text{eff}}$  calculation is here mainly dependent on NOx content. Future studies should try to investigate this issue for lightning emissions mixed with strong surface emissions in order to sharpen our parameterization”

4. *I would expect lightning plumes to be highly efficient PAN producers, since the convection in which lightning occurs would also loft short-lived peroxyacetyl radicals from the surface to react with the elevated NOx, and the temperatures in the cold free and upper troposphere will guarantee that PAN does not thermally decompose and it will outlast the plume. However, because the plume formulation does not allow NOx to be converted into PAN in the plume, it is released as NOx away from the regions of elevated peroxyacetyl radicals, and therefore global PAN decreases, as the authors correctly explain in Section 4. However, unless the ratio of PAN production to HNO3 production is relatively suppressed in the high-NOx plumes (which I would not expect), then this is likely an error in the PAN budget introduced by the plume parameterization. I think the authors should comment based on their DSMACC results whether relative PAN production is stable, enhanced or suppressed in the high-NOx conditions. Unless it is suppressed, then I think that a conclusion of this paper should be a recommendation that future studies with a similar lightning plume parameterization include an additional  $\beta$  term that characterizes the conversion of NOx to PAN, and associated  $d[\text{PAN}]/dt$  and  $d[\text{CH}_3\text{C}(\text{O})\text{OO}]/dt$  continuity equations alongside those for HNO3, O3, and NOx.*

This is an excellent comment from the referee#3. As showed in the manuscript, our LNOx plume parameterization implies a decrease in PAN mixing ratio at global scale, which is mainly explained by the storage of NOx in the plume form along the transport.

The following two figures show  $d[\text{PAN}]/dt$  and  $d[\text{HNO}_3]/dt$  implied by high NO concentration (0.7ppb, 3.42ppb and 10ppbb) as results from DSMACC box model simulations (example for the mid-latitudes conditions at daytime). These figures show that high NO condition implies a significant increase in PAN, which is higher by a factor  $10^5$  than the HNO3 production.



Therefore, we agree with the referee#3 about the potential gap for PAN chemistry in our LNO<sub>x</sub> plume parameterization. It could be of great interest to add the PAN and CH<sub>3</sub>C(O)OO continuity equations and a new term to describe the NO<sub>x</sub> conversion to PAN within the plume.

A discussion about the PAN chemistry was added in the manuscript, in section 4.2.2, as follows: “Note that the production of PAN is limited by the supply of NO<sub>x</sub> or non-methane volatile organic compounds (NMVOCs). Above continental lightning sources regions, NMVOCs are uplifted by deep convection but with lower NO<sub>x</sub> due to the activation of the plume parameterization. That implies a less efficient PAN production in these regions. Downwind of lightning sources regions (oceanic regions), NO<sub>x</sub> increases because of the LNO<sub>x</sub> transport in the plume form but there is less NMVOCs available to produce PAN. Therefore, both in regions of LNO<sub>x</sub> emissions and downwind the PAN production is limited leading to overall lower PAN mixing ratios at large scale in P1 experiment. However, this may be nuanced by considering the PAN chemistry in future studies using similar LNO<sub>x</sub> plume parameterization by introducing the PAN and CH<sub>3</sub>C(O)OO continuity equations and a new term to consider the fraction of NO<sub>x</sub> converted to PAN within the plume. This should allow the PAN production during the plume transport, which is inhibited in the current version.”

Specific comments:

- \* *P34093, L7-13: Only some lightning NO<sub>x</sub> is detrained in the cloud anvil, much is detrained at lower altitudes during the convective updrafts and downdrafts as seen in the Ott et al. (2010) profiles. I would rephrase this sentence to be “Most NO<sub>x</sub> produced by lightning is detrained into the free and upper troposphere, where ozone production efficiencies (OPE) per unit NO<sub>x</sub> emitted are 4 to 20 times higher than at the surface (refs), and therefore lightning exerts a disproportionately stronger effect on photochemistry than surface emissions (refs).”*

We agree with the referee suggestion. This has been changed in the revised version of the manuscript.

- \* *P34093, L21-23: Recommend changing the start of the sentence to “Therefore, lightning NO<sub>x</sub> production must be parameterized for inclusion...”*

This has been changed in the revised version of the manuscript.

- \* *P34093, L26-27: LIS and OTD are currently the only options, and OTD was not on the TRMM satellite.*

We agree with the referee comment and we have change the sentence as follows: “Flashes simulated by CTMs are commonly constrained by satellite observations (Sauvage et al., 2007b; Murray et al., 2012) from the space-borne Lightning Imaging Sensor (LIS) on TRMM and the Optical Transient Detector (OTD) (Christian et al., 2003; Tost et al., 2007).”

- \* *P34094, L1: Many models now use newer vertical distribution profiles from Ott et al. (2010), including GEOS-Chem, which are “reverse-C”-shaped, so please update the text here and elsewhere.*

This has been changed in the revised version of the manuscript.

- \* P34094, L6: *I would recast as “Despite the necessity of including lightning NO<sub>x</sub> emissions in global models, ...”*

This has been changed in the revised version of the manuscript.

- \* P34094, L15: *Please change “realistic” to “more realistic”, as the plume scheme is still a parameterization (and similarly in P34118, L18; P34121, L5; P34123, L27).*

This has been changed in the revised version of the manuscript.

- \* P34096, L13-14: *Heterogeneous reactions occur on all aerosol types in GEOSChem, not just sulfate and mineral dust.*

This has been changed in the revised version of the manuscript.

- \* P34096, L18: *Suggest replacing “specially estimate for” with “overwrite those for the”*

This has been changed in the revised version of the manuscript.

- \* P34096, L20: *“Fossil fuel” should be “Biofuel”*

This has been changed in the revised version of the manuscript.

- \* P34096, L22: *Lobert et al. is not a GFED reference (see doi:10.5194/acp-10-11707-2010)*

We have changed the reference related to the GFED inventory in the text.

- \* P34096, L25-P34097, L2 - *I recommend rephrasing the GEOS-Chem description to follow the order of the steps taken in the model to calculate NO<sub>x</sub> from lightning: (1) flash rates are calculated in active deep convection using the Price and Rind scheme, (2) flash rates are adjusted with local scaling factors to match the satellite climatology, (3) total column emissions are determined using NO<sub>x</sub> yields that differ in tropics and northern extratropics, and (4) total column is distributed vertically using the Ott profiles. I would also mention that the base lightning NO<sub>x</sub> scheme is described in detail by Murray et al. (2012). Have the authors made any additional modifications to the standard GEOS-Chem implementation for their base case (BC) simulation, or does that simulation use GEOS-Chem as is publicly released?*

We thank the referee#3 for his/her suggestion. In this present study, there is no additional change to the standard GEOS-Chem implementation related to the BC experiment. This has been changed in the revised version of the manuscript, in the section 2.1, as follows:

“In order to calculate the NO<sub>x</sub> from lightning, flash rates are first calculated in active deep convection using the Price and Rind Scheme based on the cloud-top-height (Price and Rind, 1992, 1994), then flash rates are adjusted with local scaling factors to match the satellite climatology (Sauvage et al., 2007b; Murray et al., 2012), and the total column emissions are determined using NO<sub>x</sub> yields that differ in tropics and northern extratropics. Finally, the total column is distributed vertically using the reverse C-shaped profile from Ott et al. (2010). Note

that the base lightning NO<sub>x</sub> scheme is described in detail by Murray et al. (2012)."

- \* P34098, L22-23: *Please give the mass of the LNO<sub>x</sub> tracer used, and specify whether or not it varies in space and time (as the mean mass of NO<sub>x</sub> does due to changes in NO/NO<sub>2</sub> ratios).*

The initial LNO<sub>x</sub> tracer mass corresponds to the NO<sub>x</sub> mass at the time of the beginning of the simulation within the GEOS-Chem model. However, the LNO<sub>x</sub> tracer is considered as a passive tracer within the model following the monotonic exponential decay applied by the plume parameterization. We have clarified this point in the manuscript as follows:

"Following Cariolle et al. (2009), a passive tracer (from the perspective of the usual model chemistry) is added to the CTM to represent NO<sub>x</sub> emitted by lightning. The LNO<sub>x</sub> tracer initial mass corresponds to the NO<sub>x</sub> mass at the start time of the simulation. Rather than increasing the concentration of NO<sub>x</sub> within the CTM, lightning NO<sub>x</sub> emissions now increase the concentration of this new passive tracer, which is transported in the standard way by advection and turbulence. Plume chemistry is considered to be significant when the mixing ratio of the lightning NO<sub>x</sub> tracer is higher than a critical NO<sub>x</sub> content, hereafter denoted  $r_l$ . Above this value the lightning NO<sub>x</sub> tracer is transferred to the normal NO<sub>x</sub> tracer at a rate described by a plume lifetime ( $\tau$ ), which is an exponential decay constant. This corresponds to an exchange time scale between the lightning NO<sub>x</sub> plume and the background NO<sub>x</sub>."

- \* P34099, L13: *I should be the injection rate of "LNO<sub>x</sub>", and the units used here should be the same in P34113, L21.*

This has been changed in the revised version of the manuscript.

- \* P34100, L17-20 - *Equation (4) includes  $\text{NO}_x$  and  $\text{ElNO}_x$ . However, later in the text it is stated that these values are 1, which is non-physical based on what they are supposed to represent. However, the "fuel" tracer in this case is comprised only of NO<sub>x</sub>, so I believe the authors should just remove  $\text{NO}_x$  and  $\text{ElNO}_x$  everywhere from this work as superfluous (as long as the molecular mass of the LNO<sub>x</sub> tracer is specified). If they prefer to leave them in, please state what the g (N, NO, NO<sub>2</sub>, NO<sub>x</sub>?) and kg (air, LNO<sub>x</sub>?) are referring to in  $\text{ElNO}_x$ .*

We agree with the suggestion of the referee#3. The  $\text{ElNO}_x$  variable has been removed from the equations.

- \* P34101, L4-5: *Ozone is still an order of magnitude greater.*

We thank the referee for his/her comment and the sentence has been change in the text as follows:

"In the case of large NO<sub>x</sub> injection by lightning, the NO<sub>x</sub> content (~40 ppt in unpolluted atmosphere) becomes close (a few ppb, according to in-situ measurements, Dye et al. (2000); Huntrieser et al. (2002)) to the surrounding ozone (60±24 ppb) (Jaéglé et al., 1998)."

- \* P34101, L13-14: Recommend replacing “The sums of the concentrations as detailed by the Eqs. (5)-(7)” with “The rate of change of each chemical family are given by Eqs. (5)-(7)”.

This has been changed in the revised version of the manuscript.

- \* P34102, L24-P34103, L2: It is given here that  $K_{eff}$  is a function of the plume concentrations of  $NO_x$  and  $O_3$ , but the C09 derivation uses only in-plume  $NO_x$  concentrations and background  $O_3$  concentrations in its definition of  $K_{eff}$ . Please clarify what is used here and correct the integrals as necessary.

In the  $K_{eff}$  equation,  $r_{NO_x}^P$  and  $r_{O_3}^P$  correspond to the mixing ratios of  $NO_x$  and  $O_3$  respectively in the plume and the overlined  $r_{O_3}$  term is the background ozone mixing ratio averaged in the model grid as described in Cariolle et al., 2009. We have clarified this point in the text.

- \* P34103, L17-P34104 L18: Please add “primarily” to the discussion of the day and night reactions, since both reactions occur both at day and night. Please clarify what is meant by “characterized by the coefficient  $\beta$ ” (I assume molar fraction of  $NO_x$  converted to  $HNO_3$ ?).

We have clarified this point in the text as follows: “In addition, we consider the conversion of  $NO_x$  into  $HNO_3$  within the plume. This conversion takes place in two different ways depending on the day or night atmospheric conditions. During the day,  $NO_2$  reacts primarily with  $OH$  to give  $HNO_3$  directly and it is characterized by the coefficient  $\beta_1$ . While at nighttime the conversion of  $NO_x$  to  $HNO_3$  occurs mainly through  $N_2O_5$  formation followed by a heterogeneous hydrolysis reaction, which corresponds to  $\beta_2$ . In other words, the  $\beta$  coefficients are the molar fractions of  $NO_x$  converted to  $HNO_3$  within the plume. These two fractions are unitless”.

- \* P34104, L15: It is somewhat misleading to include PAN here. It is true that PAN is forming in the box model used to calculate  $\beta_1$  and  $\beta_2$ , therefore reducing the magnitude of those values by preventing some  $NO_x$  from being converted to  $HNO_3$ . However, the plume parameterization does not include a  $d[PAN]/dt$  equation, nor does  $d[NO_x]/dt$  include any losses associated with PAN production in the plume, so this PAN remains as  $NO_x$  as far as GEOS-Chem is concerned.

We agree with the referee#3 comment. PAN has been removed here.

- \* P34106, L23-24: Recommend changing to “related to highly elevated  $NO_x$  concentrations relative to the background”.

This has been changed in the revised version of the manuscript.

- \* Section 3.2.1:  $D_h$  was only estimated for outflow from deep convective anvils, but a lot of lightning  $NO_x$  is released beneath the anvil. Please clarify if a constant  $D_h$  was used in all plumes, and didn't vary with altitude or latitude?

We agree with the referee, that  $LNO_x$  may be released beneath the anvil. Three different values of  $D_h$  [0.1; 15; 100]  $m^2.s^{-1}$  were estimated in our study. The first value  $D_h=0.1 m^2.s^{-1}$  was obtained from in situ measurements outside the anvil but close to this region and could be related to the plume from beneath the anvil. The second value,  $D_h=15 m^2.s^{-1}$  was obtained from

measurements within the anvil region. Finally the last value,  $D_h=100 \text{ m}^2\cdot\text{s}^{-1}$  corresponds to the horizontal diffusion in the anvil and was obtained from a convective cell simulation with Meso-NH.

From these estimates, we have a first guess of  $D_h$  in the anvil but also outside and close to the anvil from two different approaches. In this study,  $D_h$  is constant for each experiment performed with the GEOS-Chem model.  $D_h$  is used in the simple dispersion model (new section 2.4) in order to determine the plume lifetime and  $K_{\text{eff}}$  but this parameter does not appear directly in our parameterization in the GEOS-Chem model. As discussed before in response to the referee#1, although it is very relevant, the global variability of  $D_h$  was not studied here because it is not solve at large scale by the GEOS-Chem model. We may expect that  $D_h$  varies mainly with altitude and also latitude. Further modeling studies and in situ measurements should be performed in the future to better understand this parameter variability at large scale and improve the characterization of the LNO<sub>x</sub> plume dispersion.

We have clarified this point in the revised version of the manuscript in section 3.2.1, as follows: "In order to cover all horizontal diffusivity estimates discussed in this section the range of values 0.1, 15 and  $100 \text{ m}^2 \cdot \text{s}^{-1}$  was used. The horizontal coefficient is constant for all lightning NO<sub>x</sub> plumes considered in the GEOS-Chem model. Hereafter, the results are detailed for the central value  $D_h = 15 \text{ m}^2 \cdot \text{s}^{-1}$ ."

- \* P34107, L5-7: *"defined" would be better as "determined"? Please clarify what is meant by "mainly from previous in-situ measurement in thunderstorm anvil".*

We agree with the referee comment. By the sentence *"mainly from previous in-situ measurement in thunderstorm anvil"*, we would highlight that the  $D_h$  estimate from in-situ measurements may be the most accurate. The  $D_h$  estimate related to this method is more realistic (in agreement with Cariolle et al., 2009,  $D_h$  estimate) than the estimate from the modeling study. This has been removed in this paragraph but it is mentioned after in this section.

This has been change in the revised version of the manuscript in section 3.2.1, as follows: "The diffusion coefficient was determined by two different ways. A first estimate of the horizontal diffusion was performed by running the 3-D mesoscale Meso-NH model. Then, the  $D_h$  coefficient was calculated using in-situ measurements in thunderstorm anvil".

- \* P34107, L12: *"performed" would be better than "made"*

This has been changed in the revised version of the manuscript.

- \* P34107, L17: *If e is not Euler's constant, please define.*

The "e" is the exponential function here. It has been replaced by "exp" in the revised manuscript.

- \* P34109, L17-23: *How are the tropics vs. midlatitudes defined when rl is applied in the model?*

The critical content mixing ratio  $rl$ , above which the  $LNO_x$  plume exists, is used in the plume dispersion model in order to estimate the plume lifetime ( $\tau$ ) and  $K_{eff}$ . In these dispersion simulations, the tropics and the mid-latitudes conditions are distinguished using initial concentrations for chemical species relative to the two latitude regions (Table 1). From these runs, we got different values for  $\tau$  (and  $K_{eff}$ ). Finally, in GEOS-Chen model, the  $\tau$  values are applied depending on the latitude region.

- \* P34110, L1: Please clarify what is meant by “an ensemble of spikes”

In our parameterization, each  $LNO_x$  plume is associated with several electrical discharges at the convective cell scale. We have clarified this point in section 3.2.3, as follows:

“Here we use a width of 500 m to refer to an ensemble of spikes at cloud scale (i.e. each plume is defined from several electrical discharges associated with a convective cell).”

- \* P34111, L2: Please replace “defined” with “estimated”

This has been changed in the revised version of the manuscript.

- \* P34111, L4: *Is it appropriate to use separate  $rl$  for night and day, when some of the lifetimes are much longer than 12 hours? Why wouldn't we just use the smaller of the two values in both day and night?*

There is some plume lifetimes longer than 12 hours but most are shorter (67 %). Also, there is a significant difference in the plume lifetime between day and night (Table 2). For example, for  $NO_i^{max}$  there is 3.6 hours and 13.6 hours difference in the mid-latitudes and tropics respectively. We cannot consider only the smallest value of  $rl$  because this could imply longer lifetime, which is less realistic than the use of the  $rl$  day and night distinguish values.

- \* P34111, L24-25: Please clarify the sentence so it is clear whether it is meant that  $K_{eff}$  is “very low” relative to the C09 values or the background  $K$  values?

This has been clarified in the revised version of the manuscript in section 3.2.4, as follows: “Our  $K_{eff}$  estimates are smaller than those calculated by Cariolle et al. (2009) for the plume chemistry related to aircraft exhausts. In this previous work,  $K_{eff}$  varies from 1.0 to  $4.2 \cdot 10^{-18}$  molecules $^{-1} \cdot s^{-1} \cdot cm^3$  with a mean value close to  $3 \cdot 10^{-18}$  molecules $^{-1} \cdot s^{-1} \cdot cm^3$  depending on the  $NO_x$  loading.”

- \* P34113, L23: I think “undiluted” should be “diluted” here

The use of the “undiluted” term is the good choice here. In fact, in our plume parameterization, the mixing ratio of the tracer ( $\Gamma_{LNO_x}$ ) represents the  $NO_x$  mixing ratio from lightning emissions. In other words, this is the  $NO_x$  in the plume form not yet released to the model grid as a background concentration.

- \* P34113, L24: *Lightning does produce some  $NO_2$  (as well as other species). I would change to “lightning produces negligible quantities of  $NO_2$  relative to  $NO$  and therefore  $E$  is effectively 0 in Eq. (15).”*



This has been changed in the revised version of the manuscript.

- \* P34116, L5: *“produced” (not reproduced). I would refer to the altitudes in Fig. 3c as “middle and upper troposphere” as the tropopause is ~70 mb in the tropics.*

This has been changed in the revised version of the manuscript as follows: “The lightning NO<sub>x</sub> tracer is produced at altitudes where lightning NO<sub>x</sub> are calculated and detrained (in the upper troposphere, between ~500 and 300 hPa) as shown in panels (c) in figure 3.”

- \* P34117 L6: *Should be “volatile”*

This has been changed in the revised version of the manuscript.

- \* Sections 4.3.1-4.3.2: *Here the word “variability” would be better replaced by “sensitivity”, and all the various \_O3 and \_NOx values referred to as “ranges” or “changes” associated with the uncertainty in the different explored parameters examined.*

This has been changed in the revised version of the manuscript.

P34121, L1: *“significant” should probably be “large” here.*

This has been changed in the revised version of the manuscript.

- \* Figure 1: *This diagram needs a longer caption to describe what the lines, arrows, boxes, and colors represent. I would recommend removing the boxes from around the “[NO<sub>x</sub>] < r<sub>l</sub>” and “[NO<sub>x</sub>] > r<sub>l</sub>” to make it clear that those are a conditional statements (also, [NO<sub>x</sub>] should probably be [LNO<sub>x</sub>] there), and move the edge of the green “ERR” box to the other side of the conditional.*

This has been changed in the revised version of the manuscript.

- \* Figures 3-7: *I was originally confused because I interpreted these captions as that Dh and NO<sub>i</sub> were somehow applied in GEOS-Chem, not that the  $\tau$  and K<sub>eff</sub> values were trained from the offline simple plume dispersion model using those Dh and NO<sub>i</sub> values. I would recommend rephrasing to make that distinction clearer.*

This has been changed in the revised version of the manuscript.

# Modeling lightning- $NO_x$ chemistry at sub-grid scale in a global chemical transport model

Alicia Gressent<sup>1</sup>, Bastien Sauvage<sup>1</sup>, Daniel Cariolle<sup>2,3</sup>, Mathew Evans<sup>4</sup>,  
Maud Leriche<sup>1</sup>, Céline Mari<sup>1</sup>, and Valérie Thouret<sup>1</sup>

<sup>1</sup>LA, CNRS, Université de Toulouse, Toulouse, France

<sup>2</sup>Météo France, Toulouse

<sup>3</sup>Centre Européen de Recherche et de Formation Avancée en Calcul Scientifique, CERFACS, Toulouse

<sup>4</sup>The Wolfson Atmospheric Chemistry Laboratories, University of York, UK

*Correspondence to:* Alicia Gressent (alicia.gressent@aero.obs-mip.fr)

**Abstract.** For the first time, a plume-in-grid approach is implemented in a chemical transport model (CTM) to parameterize the effects of the non-linear reactions occurring within high concentrated  $NO_x$  plumes from lightning  $NO_x$  emissions ( $LNO_x$ ) in the upper troposphere. It is characterized by a set of parameters including the plume lifetime, the effective reaction rate constant related to  $NO_x$ - $O_3$  chemical interactions and the fractions of  $NO_x$  conversion into  $HNO_3$  within the plume. Parameter estimates were made using the DSMACC chemical box model, simple plume dispersion simulations and the mesoscale 3-D Meso-NH model. In order to assess the impact of the  $LNO_x$  plume approach on the  $NO_x$  and  $O_3$  distributions at large scale, simulations for the year 2006 were performed using the GEOS-Chem global model with a horizontal resolution of  $2^\circ \times 2.5^\circ$ . The implementation of the  $LNO_x$  parameterization implies  $NO_x$  and  $O_3$  decrease at large scale over the region characterized by a strong lightning activity (up to 25 % and 8 %, respectively, over Central Africa in July) and a relative increase downwind of  $LNO_x$  emissions (up to 18 % and 2 % for  $NO_x$  and  $O_3$ , respectively, in July) are derived. The calculated variability of  $NO_x$  and  $O_3$  mixing ratios around the mean value according to the known uncertainties on the parameter estimates is maximum over continental tropical regions with  $\Delta NO_x$  [-33.1; +29.7] ppt and  $\Delta O_3$  [-1.56; +2.16] ppb, in January, and  $\Delta NO_x$  [-14.3; +21] ppt and  $\Delta O_3$  [-1.18; +1.93] ppb, in July, mainly depending on the determination of the diffusion properties of the atmosphere and the initial  $NO$  mixing ratio injected by lightning. This approach allows (i) to reproduce a more realistic lightning  $NO_x$  chemistry leading to better  $NO_x$  and  $O_3$  distributions at the large scale and (ii) focus on other improvements to reduce remaining uncertainties from processes related to  $NO_x$  chemistry in CTM.

## 1 Introduction

Lightning emissions are one of the most important sources of nitrogen oxides ( $NO_x \equiv NO + NO_2$ ) in the upper troposphere (WMO, 1999; Hudman et al., 2007). Lightning ~~emitted~~ primarily produce

~~NO and may also induce a negligible quantity of  $NO_2$  with a ratio  $NO_2/NO_x$  of 0.5 to 0.1~~

25 ~~(Franzblau, 1991; Stark et al., 1996).  $NO_x$  emitted by lightning ( $LNO_x$ ) impact the tropospheric~~  
~~ozone burden (Stockwell et al., 1999; Hauglustaine et al., 2001; Grewe, 2007), and the hydroxyl-~~  
~~radical (OH) concentrations influencing the oxidizing capacity of the atmosphere (Labrador et al.,~~  
~~2004; Banerjee et al., 2014). Lightning flashes including cloud-to-ground and intra-cloud flashes~~  
~~produce reactive nitrogen species which are detrained in the cloud anvil (Weiss et al., 2012) and~~  
30 ~~released directly in the upper troposphere. Because of an ozone production efficiency~~  
~~Most  $NO_x$~~   
~~produced by lightning is detrained into the free and upper troposphere, where ozone production~~  
~~efficiencies (OPE) per unit  $NO_x$  emitted are 4 to 20 times larger in the upper troposphere than~~  
~~in the middle or low troposphere (Sauvage et al., 2007a; Martin et al., 2007), effects of  $LNO_x$  on~~  
~~chemistry are expected to be stronger in the upper troposphere higher than at the surface (Sauvage et al., 2007a; Martin et al., 2007),~~  
35 ~~and therefore lightning exerts a disproportionately stronger effect on photochemistry than surface~~  
~~emissions (Pickering et al., 1990; Hauglustaine et al., 1994; Zhang et al., 2003; Choi et al., 2009).~~  
The longer  $NO_x$  lifetime in the upper troposphere (1-2 weeks) allows the long-range transport of  
 $LNO_x$  through the large circulation patterns (Hemispheric Transport of Air Pollution, HTAP report,  
2010: <http://www.htap.org/>).

40 Although the importance of the  $LNO_x$  emissions on the upper tropospheric chemistry is well  
known, it remains highly uncertain with a best estimate of  $2-8 \text{ TgN} \cdot \text{yr}^{-1}$  (Schumann and Huntrieser,  
2007). Lightning  $NO_x$  emissions are associated with deep convection (horizontal scale  $\sim 10 \text{ km}$ )  
and correspond to the "sub-grid" in global chemical transport models (horizontal resolution  $\sim 100 \text{ s}$   
km). ~~This implies that the impact of the~~ ~~Therefore,~~ lightning  $NO_x$  ~~emissions should~~ ~~production must~~  
45 be parameterized for inclusion into a large scale model. Global models commonly used convection  
proxies such as the cloud-top-height (Price and Rind, 1992) and the updraft intensity to estimate the  
lightning flashes. Flashes simulated by CTMs are commonly constrained by satellite observations  
(Sauvage et al., 2007b; Murray et al., 2012) ~~such as measurements~~ from the space-borne Lightning  
Imaging Sensor (LIS) ~~on TRMM~~ and the Optical Transient Detector (OTD) ~~on TRMM~~ (Christian  
50 et al., 2003; Tost et al., 2007). The lightning  $NO_x$  emissions are then redistributed according to a  
vertical profile generally a ~~reverse~~ "C-Shape" profile (~~Pickering et al., 1998~~) (~~Ott et al., 2010~~) a pri-  
ori defined depending on season, latitude and continent/ocean location. Also, corrections on the  
calculations of lightning  $NO_x$  emissions using satellite observations (SCIAMACHY, Martin et al.  
(2007)) and in-situ measurements (INTEX-NA, Hudman et al. (2007)) are usually applied.

55 Despite the ~~success in simulating the~~ ~~necessity of including~~ lightning  $NO_x$  emissions ~~in global~~  
~~models,~~ the small scale nature of the flashes and the non-linear chemistry (Lin et al., 1988) of the  
atmosphere will lead to biases on the large scale with instantaneous dilution of gases in the large  
grid box volume. It seems likely that this will lead to an overestimate of the OPE and an underesti-  
60 mate of the nitric acid ( $HNO_3$ ) production. For instance, by forcing  $NO_x$  concentration in GEOS-

Chem grid box over Southeast Asia to represent the measured lightning plumes, Cooper et al. (2014) ~~estimate~~-estimated a ratio for  $O_3$  to  $HNO_3$  produced leading to a 15  $mol/mol$  OPE in lightning plumes, that reinforces the fact that instantaneous dilution in global model implies issues in sub-grid chemistry.

65

In this work, a more realistic lightning  $NO_x$  chemistry as well as a plume parameterization is implemented into a global chemical transport model (CTM) allowing reproducing more accurately the ~~large-scale~~- $NO_x$  and  $O_3$  ~~distribution~~distributions at large scale. The plume approach used in this study was previously developed by Cariolle et al. (2009) for aircraft  $NO_x$  emissions in the LMDz-  
70 INCA and MOBIDIC models and also implemented to deal with the ship  $NO_x$  emissions (Huszar et al., 2010). This approach avoids the double count in the CTM calculation of the emitted  $NO_x$ , first instantaneously diluted into the point grid and ~~second~~-secondly as the plume form. In addition, the plume parameterization is the first that considers the  $NO_x$  from lightning as a plume with the transport of the related non-linear chemistry effects.  $NO_x$  from lightning emissions are emitted in  
75 the upper troposphere characterized by strong winds ~~that allows~~-allowing the large scale transport of trace species. Thus, it is relevant to consider a plume growth from lightning emissions, which could be diluted long time after the initial lightning pulse, downwind of emissions. Consequently, the plume parameterization previously developed for aircraft exhausts has been adjusted to  $LNO_x$  emissions and implemented into the GEOS-Chem global chemical transport model.

80

Section 2 gives a description of the GEOS-Chem model in which the plume-in-grid parameterization is implemented and ~~models~~-the models which are used to evaluate the diffusion properties of the atmosphere and to determine parameters characterizing the physics and chemistry of the lightning  $NO_x$  plume. A concise description of the plume approach is then presented in section 3 followed  
85 by a detailed explanation of the determination of parameters related to  $LNO_x$  emissions. Section 4 summarizes the results of the simulations performed with GEOS-Chem and finally these results and the sensitivity on  $NO_x$  and  $O_3$  variations of the parameterization are discussed in section 5.

## 2 Models

Three different models are used in this evaluation and are described in this section. GEOS-Chem  
90 is used to provide a global framework to assess the impact of lightning  $NO_x$ . Meso-NH is used to provide estimates of the plume diffusion timescales and DSMACC is a box model used to assess the non-linear chemistry in the plume.

## 2.1 The GEOS-Chem chemical transport model

The GEOS-Chem chemical transport model (Bey et al., 2001) is a global 3-D model of atmospheric composition driven by assimilated meteorology from the Goddard Earth Observing System (GEOS-5) of the NASA Global Modeling Assimilation Office (GMAO). The 09-01-01 version ([http://wiki.seas.harvard.edu/geos-chem/index.php/GEOS-Chem\\_v9-01-01](http://wiki.seas.harvard.edu/geos-chem/index.php/GEOS-Chem_v9-01-01)) of the CTM has been used in this study. The model transports 43 tracers to describe tropospheric  $O_3$ - $NO_x$ -VOC chemistry. The horizontal resolution is  $2^\circ \times 2.5^\circ$  and 47 vertical levels are defined from the ground to 80 km altitude. The CTM includes modules for emissions, transport, chemistry, deposition, aerosols and surface.

The large-scale advection of tracers is performed using the TPCORE advection scheme (Lin and Rood, 1996) corresponding to a semi-lagrangian flux method. Shallow and deep moist convection processes are carried out using the Relaxed Arakawa-Schubert scheme (Moorthi and Suarez, 1991). Mixing in the lower atmospheric layers is represented by a non-local scheme of the planetary boundary layer described by Lin and McElroy (2010). The wet deposition for water-soluble aerosols and for gases follows Liu et al. (2001) and Amos et al. (2012). Aerosol scavenging by ice crystals and cold/mixed precipitation is also reproduced in the model (Wang et al., 2011). The dry deposition is associated to a scheme which calculates bulk surface resistance in series (Wesely, 1989). Photolysis rates are calculated with the Fast-JX code (Bian and Prather, 2002). The atmospheric chemistry is resolved using the SMVGEAR solver (Jacobson and Turco, 1994) with more than 300 species and 785 chemical reactions. Heterogeneous chemical reactions are represented on the surface of ~~the sulfate aerosols (Bey et al., 2001) and mineral dust (Martin et al., 2002)~~ aerosols (Bey et al., 2001; Martin et al., 2002). Effects of aerosols on the photolysis rates are based on Martin et al. (2003). Primary  $NO_x$  and VOCs (Volatile Organic Compounds) emissions are separated depending on sources. Global anthropogenic emissions are given by the GEIA (Wang et al., 1998) and EGDAR (Olivier, 2005) inventories and regional anthropogenic emissions are ~~specifically estimate~~ for overwrite those for the US (NEI05), Canada (CAC), Mexico (BRAVO), Europe (EMEP) and East Asia (Streets et al., 2006; Zhang et al., 2009). ~~Fossil-fuel~~ Biofuel emissions are provided by EPA and STREETS 2006 inventories (Yevich and Logan, 2003), biomass burning emissions by GFED inventory (~~Robert et al., 1999~~) (van der Werf et al., 2010), and biogenic emissions by the MEGAN model calculations (Guenther et al., 2012). In addition,  $NO_x$  from soil emissions are calculated by an algorithm depending on temperature and precipitation (Yienger and Levy, 1995).

~~The lightning~~ In order to calculate the  $NO_x$  ~~emissions calculation is initially from lightning, flash rates are first calculated in active deep convection using the Price and Rind Scheme based on the cloud-top-height parameterization (Price and Rind, 1992, 1994) with a "~~ (Price and Rind, 1992, 1994), then flash rates are adjusted with local scaling factors to match the satellite climatology (Sauvage et al., 2007b; Murray et al., 2012).

130 and the total column emissions are determined using  $NO_x$  yields that differ in tropics and northern  
extratropics. Finally, the total column is distributed vertically using the reverse C-shaped "profile  
describing  $LN O_x$  vertical distribution (Pickering et al., 1998; Ott et al., 2010). Lightning flashes are  
constrained using the climatologies from the LIS/OTD observations (Sauvage et al., 2007b; Murray et al., 2012).  
Global profile from Ott et al. (2010). Note that the base lightning  $NO_x$  emissions are also constrained  
135 to  $6 \text{ Tg N yr}^{-1}$  in order to match to satellite observations (Martin et al., 2007). scheme is described  
in detail by Murray et al. (2012).

## 2.2 The Meso-NH model

The Meso-NH model is an atmospheric model developed jointly by the Laboratoire d'Aérodynamique and  
by CNRM-GAME (<http://mesonh.aero.obs-mip.fr/mesonh51>). The model includes a non-hydrostatic  
140 and anelastic system of equations (Lafore et al., 1998) and has a complete set of parameterizations  
allowing to reproduce physical processes such as radiation (Gregory et al., 2000), atmospheric turbu-  
lence (Cuxart et al., 1999), convection (Bechtold et al., 2000), microphysics related to warm clouds  
(Cohard and Pinty, 2000), and atmospheric ice (Pinty and Jabouille, 1999; Lascaux et al., 2006).  
Meso-NH includes also on-line chemistry (Tulet et al., 2003, 2006). The model deals with large  
145 (synoptic) to small (large eddy) scales. In this study, the Mesonh-49 version was used in order to  
compare the horizontal diffusion coefficient ( $D_h$ ) estimate within the anvil of thunderstorms from  
in-situ measurements to a modeling ideal case of a convective cell.

## 2.3 The DSMACC chemical box model

The Dynamical Simple Model of Atmospheric Chemical Complexity (DSMACC) is a simple box  
150 model developed for improving our understanding of the tropospheric chemistry (Emmerson and  
Evans, 2009). The model is composed of the KPP chemical pre-processor (Damian et al., 2002) to  
solve differential equations representing the chemical system. The TUV (Tropospheric Ultraviolet  
and Visible Radiation Model) photolysis scheme is used, which calculates the spectral irradiance,  
the spectral actinic flux, photodissociation coefficients (J-values) (Madronich and Flocke, 1999),  
155 and biologically effective irradiance. The chemical scheme used derives from the Master Chemi-  
cal Mechanism (MCM, <http://mcm.leeds.ac.uk/MCM/>), (Jenkin et al., 1997; Saunders et al., 2003),  
which contains 17000 elementary reactions of 6700 primary, secondary and radical species.

In order to study the chemical interactions that could occur in the undiluted plume fraction, a set  
160 of short simulations was carried out with the DSMACC chemical box model as explained in the  
section 3.2.2.

## 2.4 The simple plume dispersion model

To model the dispersion of lightning  $NO_x$  emissions we use a simple dispersion model similar to the plume model used for aircraft  $NO_x$  emissions, except that the plume is supposed to be oriented along a vertical axis. The plume is represented as a cylinder that encompass horizontal diffusion with a constant coefficient  $D_h$  (section 3.2.1). This simple model is composed of 30 horizontal circles with spacing increasing progressively from the center axis. The discretization of the diffusion equation is mass conservative.

The chemistry scheme and associated reaction rate constants is adapted from the large-scale chemical model MOCAGE (Teyss  re et al., 2007). It includes the main reactions involved in the  $NO_x - HO_x$  system. Simple plume simulations were performed in order to estimate the physical and chemical characteristics of the plumes related to lightning  $NO_x$  emissions.

### 3 Plume parameterization for lightning $NO_x$ emissions

#### 3.1 General description

The  $LNO_x$  plume parameterization is based on a method initially developed by Cariolle et al. (2009) for  $NO_x$  emissions related to aircraft exhausts later adapted to ship emissions of  $NO_x$  (Huszar et al., 2010). In this approach, the plume effects at sub-grid scale are represented via a fuel tracer, to follow the amount of the emitted species in the plume and an effective reaction rate for the ozone production and nitric acid production/destruction during the plume’s dilution into the background (Cariolle et al., 2009; Paoli et al., 2011). The parameterization requires a proper estimation of the characteristic plume lifetime during which the non-linear interactions between species are important and simulated via specific rates of conversion. The approach ensures the mass conservation of species in the model. This is the only method which considers a plume evolution related to the local  $NO_x$  emissions allowing the transport of the non-linear effects occurring at smaller scale than the model grid.

##### 3.1.1 Physical plume formulation

Following Cariolle et al. (2009), a passive tracer (from the perspective of the usual model chemistry) is added to the ~~model~~-CTM to represent  $NO_x$  emitted by lightning. The  $LNO_x$  tracer initial mass corresponds to the  $NO_x$  mass at the start time of the simulation. Rather than increasing the concentration of ~~the  $NO_x$  tracer in the model~~within the CTM, lightning  $NO_x$  emissions now increase the concentration of this new passive tracer which is transported in the standard way by advection and turbulence. Plume chemistry is considered to be significant when the ~~concentration~~-mixing ratio of the lightning  $NO_x$  tracer is higher than a critical  $NO_x$  content, hereafter denoted  $r_l$ . Above this value the lightning  $NO_x$  tracer is transferred to the normal  $NO_x$  tracer at a rate described by a plume lifetime ( $\tau$ ), which is an exponential decay constant. This corresponds to an exchange time

scale between the lightning  $NO_x$  plume and the background  $NO_x$ . The continuity equation related to the tracer evolution is detailed by the equation 1.

$$\frac{\partial \overline{r_{LNO_x}}}{\partial t} + \langle F_{LNO_x} \rangle = I - \frac{1}{\tau} \cdot \overline{r_{LNO_x}} \quad (1)$$

200 Where  $\overline{r_{LNO_x}}$ , is the ~~concentration (in molecules  $\cdot cm^{-3}$ )~~ mixing ratio (in ppb) of the  $NO_x$  lightning tracer in the model grid (note that all overlined terms referred to grid average quantities in the CTM),  $F_{LNO_x} \equiv \nabla \cdot (\overline{r_{LNO_x}} u) + \nabla \cdot (D_t \nabla \overline{r_{LNO_x}})$  and it corresponds to the flux divergence related to the large-scale transport of the tracer (advection and turbulent diffusion, in ~~molecules  $\cdot cm^{-3} \cdot s^{-1}$~~  molecules  $\cdot cm^{-2} \cdot s^{-1}$ ),  $I$  is the injection rate of  ~~$NO_x$  (in molecules  $\cdot cm^{-3} \cdot s^{-1}$ )~~  $LNO_x$  (in  $s^{-1}$ ) and  $\tau$  is the plume lifetime  
205 (in seconds).

The calculation of  $\tau$  requires evaluating the mass fraction of the lightning  $NO_x$  ( $M(t)$ ) corresponding to the undiluted fraction of the plume and characterized by a  $NO_x$  ~~concentration~~ mixing ratio above the  $r_l$  critical value. In other words, the plume boundary is defined by the critical value  
210  $r_l$  depending on the time of day. The  $NO_x$  mass,  $M(t)$  decreases monotonically to zero until  $t = T_l$  for which the tracer ~~concentration~~ mixing ratio is everywhere below the  $r_l$  threshold. The plume lifetime is obtained by an exponential function depending on the mass (equations 2 and 3):

$$M(t) = \int_{V_p} \rho \cdot r_p \cdot dV \quad (2)$$

$$215 \quad \tau = \int_{t_0=0}^{+\infty} \exp(-t/\tau) \cdot dt = \frac{1}{M(t_0)} \int_{t_0=0}^{T_l} M(t) \cdot dt \quad (3)$$

Where  $V_p$  is the volume of the plume,  $\rho$  is the density of the air,  $r_p$  is the  $NO_x$  ~~concentration~~ mixing ratio within the plume (~~molecules  $\cdot cm^{-3}$  in ppb~~) and  $T_l$  is the time for which the ~~concentration~~ mixing ratio  $r_p$  is everywhere below the critical value  $r_l$ . The calculation of the plume lifetime, by simple plume dispersion simulations, depends on (i) the initial emissions of  $NO_x$  by lightning, (ii)  
220 the  $r_l$  value, and (iii) the dispersion properties of the atmosphere (related to the horizontal diffusion coefficient,  $D_h$ ) and is detailed on the section 3.2.3.

Note that the mean dispersion properties of the atmosphere were associated with the horizontal diffusion only. The lightning  $NO_x$  emissions occur in the convective part of clouds where the vertical diffusion is ~~less efficient than the horizontal one (Cariolle et al., 2009) and it is not considered in this~~  
225 ~~study. In addition~~ strong. Therefore, the vertical diffusion coefficient is a determining parameter for the  $LNO_x$  distribution in the cloud. As mentioned in section 2.1, the vertical dispersion of the plume is related to the vertical distribution of ~~distribution of the  $LNO_x$  a priori forced in the GEOS-Chem model by the C-shape profile (Ott et al., 2010) and it is beyond the scope of this study is a priori~~ calculated from Ott et al. (2010) as a reverse C-shaped profile. The  $LNO_x$  plume parameterization



230 is applied a posteriori after that lightning  $NO_x$  are vertically prescribed and concerns convective outflow where the  $NO_x$  are detrained in the troposphere. In this region of detrainment, the horizontal dispersion may be more efficient than the vertical one as it is discussed in (Cariolle et al., 2009).

### 3.1.2 Plume chemistry of $NO_x$ , $O_3$ and $HNO_3$

Once the lightning  $NO_x$  is emitted, it is transferred to model's background  $NO_x$  based on the lifetime of the plume ( $\tau$ ). Thus, the continuity equation for the  $NO_x$  species emitted in the plume and released to the large scale can be deduced as described by the equation 4.

$$\frac{\partial \overline{r_{NO_x}}}{\partial t} + \langle F_{NO_x} \rangle = + \frac{1}{\tau} \cdot \overline{r_{LNO_x}} \cdot \alpha_{NO_x} \cdot \underline{EI_{NO_x}} + L_{ss} \quad (4)$$

Where,  $\overline{r_{NO_x}}$ , is the ~~concentration-mixing ratio~~ of  $NO_x$  (~~molecules-cm<sup>-3</sup>~~ in ppb) in the model grid,  $\alpha_{NO_x}$  is the molecular mass ratio between the air and  $NO_x$  species,  ~~$EI_{NO_x}$  is the emission index for  $NO_x$  (in g/kg)~~ and  $L_{ss}$  are the large-scale sources and sinks (in ~~molecules-cm<sup>-3</sup>-s<sup>-1</sup>~~ molecules · cm<sup>-2</sup> · s<sup>-1</sup>) such as natural and anthropogenic emissions, photochemical reaction, mixing, and conversion to reservoir species.

We consider a fairly simple chemistry within the plume as described below. The increase of the nitrogen oxides concentration in the upper troposphere leads to ozone production through the reaction of  $NO$  with peroxyde ( $HO_2$ ),  $CH_3O_2$ , or  $RO_2$  radicals from the  $OH$  oxydation as shown by the reaction R1.



In the case of large  $NO_x$  injection by lightning, the  $NO_x$  content ( $\sim 40$  ppt in unpolluted atmosphere) becomes ~~of the same order close~~ (a few ppb, according to in-situ measurements, Dye et al. (2000); Huntrieser et al. (2002)) ~~than to~~ the surrounding ozone ( $60 \pm 24$  ppb) (Jaéglé et al., 1998). The ozone evolution within the plume is described by the reactions R2-R6.





From these equations we can define an  $O_x$  family ( $O_x \equiv O + O_2 + NO_2$ ,  $O_x \equiv O + O_3 + NO_2$ ) where the only net loss of  $O_x$  is by reactions between atomic oxygen and  $NO_2$  or  $O_3$ . The ~~sums of the concentrations as detailed~~ rate of change of each chemical family are given by the equations 5, 6 and 7 (Cariolle et al., 2009).

$$\frac{d(O + O_3)}{dt} = +k_2 \cdot [NO_2] - k_3 \cdot [NO] \cdot [O_3] - k_5 \cdot [O] \cdot [NO_2] - 2 \cdot k_6 \cdot [O_3] \cdot [O] \quad (5)$$

$$\frac{d(O + O_3 + NO_2)}{dt} = -2 \cdot k_5 \cdot [O] \cdot [NO_2] - 2 \cdot k_6 \cdot [O_3] \cdot [O] \quad (6)$$

$$\frac{d(NO + NO_2)}{dt} = 0 \quad (7)$$

Where  $k_i$  correspond to the rate constants for the  $R_i$  reactions.

Thus two processes occur to  $O_3$  in the plume at daytime. On short timescales  $O_x$  is conserved. Lightning emissions of  $NO$  in the plume are converted into  $NO_2$  but as  $NO_2$  is in  $O_x$  family, there is net conservation of  $O_x$ . However, on long timescales  $O_x$  can be destroyed through the reaction of  $O$  with  $NO_2$  and  $O_3$ . Both of these processes need to be considered.

The first regime (regime I) occurs at low concentrations of  $NO_x$  (relative to  $O_3$ ). Under these conditions the reaction R5 is slow. There is the rapid equilibrium between  $NO$ ,  $NO_2$  and  $O_3$  (reactions R2, R3 and R4). As a consequence,  $O_3$  is converted into  $NO_2$  and can be restored later after dilution of the plume depending on the balance between  $NO$  and  $NO_2$  at the large scale (Cariolle et al., 2009). Overall  $O_x$  is conserved. In this regime  $NO$  emitted reacts with the available  $O_3$  until the  $NO$  to  $NO_2$  ratio in the plume reaches that in the background. Thus, the impact on the  $O_3$  background concentration is to reduce it by the number of molecules of  $NO$  emitted multiplied by the background  $NO_2$  to  $NO_x$  ratio. The effect of the first regime on the ozone burden is expressed by the equation 8.

$$\frac{\partial \overline{r_{O_3}}}{\partial t} + \langle F_{O_3} \rangle = -\frac{1}{\tau} \cdot \overline{r_{LNO_x}} \cdot \alpha_{NO_x} \cdot \overline{EI_{NO_x}} \cdot \left( \frac{\overline{NO_2}}{\overline{NO_x}} - E \right) \cdot \delta + L_{ss} \quad (8)$$

Where,  $\overline{r_{O_3}}$ , is the concentration-mixing ratio of  $O_3$  (molecules-~~cm<sup>-3</sup>~~ in ppb) in the model grid,  $E$  is the  $\frac{NO_2}{NO_x}$  ratio in the initial emissions,  $\delta$  is equal to 1 during the day and 0 at nighttime,  $L_{ss}$  are the sources and sinks of ozone such as photochemical production, transport from the stratosphere,

surface deposition, photolysis reactions, and photochemical destruction.

The second regime (regime II) occurs at high concentrations of  $NO_x$  (relative to  $O_3$ ). Under these conditions the rate of R5 is large. The non-linear chemical interactions between  $NO_x$  and  $O_3$  occur with different rates than in the background atmosphere. To account for this, Cariolle et al. (2009) introduced an effective reaction rate constant ( $K_{eff}$ ), which is related to the production or the destruction of the odd oxygen ( $O_x$ ) within the plume.  $K_{eff}$  is expressed by the equation 9.

$$K_{eff} = \frac{\int_{t_0}^{T_l} (\int_{V_p} K \cdot r_{NO_x}^P \cdot r_{O_3}^P \cdot dV_p) \cdot dt}{\bar{r}_{O_3} \cdot \int_{t_0}^{t_l} (\int_{V_p} r_{NO_x}^P \cdot dV_p) \cdot dt} \quad (9)$$

Where  $r_{NO_x}^P$  and  $r_{O_3}^P$  are the ~~concentration~~ mixing ratios of nitrogen oxides and ozone within the plume,  $\bar{r}_{O_3}$  is the background ozone mixing ratio averaged in the model grid and K is the rate of  $NO_x$ - $O_3$  reaction within the plume.

The analysis of the chemical reactions related to the two regimes shows that  ~~$O_3 \gg O$  and  $k_5 \cdot NO_2$~~   $[O_3] \gg [O]$  and  $k_5 \cdot [NO_2]$  is more efficient than  ~~$k_6 \cdot O_3$~~   $k_6 \cdot [O_3]$  as a sink for  $O_x$  (Cariolle et al., 2009). Thus, the equation 6 is simplified to give the equation 10.

$$\frac{d(O_3 + NO_2)}{dt} \frac{d([O_3] + [NO_2])}{dt} = -2 \cdot k_5 \cdot [O] \cdot [NO_2] \quad (10)$$

Consequently,  $K_{eff}$  can be simplified to equation 11.

$$K_{eff} = \frac{2 \cdot (\int^T k_5 \cdot O \cdot NO_2 \cdot dt)}{(NO_x \cdot \int^T O_x \cdot dt)} \quad (11)$$

The calculation of  $K_{eff}$  is detailed in section 3.2.4. Considering the two regimes related to the sub-grid plume chemistry, the ozone burden is described by the equation 12 at daytime and nighttime. Note that at nighttime there is no direct impact due to the ozone plume chemistry on its burden as  $\delta = 0$ . Only indirect effects are expected from  $NO_y$  chemistry.

$$\frac{\partial \bar{r}_{O_3}}{\partial t} + \langle F_{O_3} \rangle = -\frac{1}{\tau} \cdot \bar{r}_{LNO_x} \cdot \alpha_{NO_x} \cdot \underline{EI_{NO_x}} \cdot \left( \frac{\bar{NO_2}}{NO_x} - E \right) \cdot \delta - K_{eff} \cdot \bar{r}_{LNO_x} \cdot \rho \cdot \alpha_{NO_x} \cdot \underline{EI_{NO_x}} \cdot \bar{r}_{O_3} \cdot \delta + L_{ss} \quad (12)$$

In addition, we consider the conversion of  $NO_x$  into  $HNO_3$  within the plume. This conversion takes place in two different ways depending on the day or night atmospheric conditions. During the day,  $NO_2$  reacts primarily with  $OH$  to give  $HNO_3$  directly and it is characterized by the coefficient  $\beta_1$ . While at nighttime the conversion of  $NO_x$  to  $HNO_3$  occurs ~~through~~ mainly through the  $N_2O_5$  formation followed by a heterogeneous hydrolysis reaction, which corresponds to  $\beta_2$ . In other words,

the  $\beta$  coefficients are the molar fractions of  $NO_x$  converted to  $HNO_3$  within the plume. These two fractions are unitless.

In summary, the equation system solved at large scale by the CTM for lightning  $NO_x$  source is detailed by the equations 13, 14 and 15.

$$\frac{\partial \overline{r_{NO_x}}}{\partial t} + \langle F_{NO_x} \rangle = + \frac{1}{\tau} \cdot \overline{r_{LNO_x}} \cdot (1 - \beta_1 \cdot \delta - \beta_2 \cdot (1 - \delta)) \cdot \alpha_{NO_x} \cdot \underline{EI_{NO_x}} + L_{ss} \quad (13)$$

$$\frac{\partial \overline{r_{HNO_3}}}{\partial t} + \langle F_{HNO_3} \rangle = + \frac{1}{\tau} \cdot \overline{r_{LNO_x}} \cdot (\beta_1 \cdot \delta + \beta_2 \cdot (1 - \delta)) \cdot \alpha_{NO_x} \cdot \underline{EI_{NO_x}} + L_{ss} \quad (14)$$

$$\frac{\partial \overline{r_{O_3}}}{\partial t} + \langle F_{O_3} \rangle = - \left( \frac{1}{\tau} \cdot \left( \frac{\overline{NO_2}}{\overline{NO_x}} - E \right) + K_{eff} \cdot \overline{r_{O_3}} \cdot \rho \right) \cdot \overline{r_{LNO_x}} \cdot \alpha_{NO_x} \cdot \underline{EI_{NO_x}} \cdot \delta + L_{ss} \quad (15)$$

Where,  $\overline{r_{NO_x}}$ ,  $\overline{r_{HNO_3}}$  and  $\overline{r_{O_3}}$ , correspond to the  $NO_x$ ,  $HNO_3$  and  $O_3$  concentrations mixing ratios averaged over the grid cell of the model, respectively.

In this study, the tropospheric chemistry and especially the  $LNO_x$  plume chemistry is considered both at daytime and nighttime since all reactions are not initiated during the day. The chemical interactions during the night correspond mainly to the reactions of  $O_3$  and  $O$  with  $NO$  and  $NO_2$  as well as the  $NO_x$  deactivation and the chemistry of the nitrogen reservoir species (here  $HNO_3$ ,  $N_2O_5$  and  $PAN$  and  $N_2O_5$ ) and the nitrate radical ( $NO_3$ ).  $NO_3$  is the main oxidant in night conditions and it is produced from the slow oxidation of  $NO_2$  by  $O_3$  (reaction R7).



The other dominant source of  $NO_3$  is the destruction of  $N_2O_5$  (reaction R8), but as  $N_2O_5$  is formed from  $NO_3$  (reaction R9), the two species act in a coupled manner.



As mentioned previously,  $N_2O_5$  is a determinant-determining species for the tropospheric chemistry at nighttime allowing the  $HNO_3$  formation by the heterogeneous reaction on the particle surface (aerosols and ice crystals). During the day,  $NO_3$  rapidly undergo-undergoes photolysis to produce  $NO$  or  $NO_2$ . In addition,  $NO_3$  reacts very quickly with  $NO$  which is more concentrated at daytime than at nighttime (reaction R10) but  $NO_3$  is very low at daytime. However, this reaction can take

place during the night especially for a plume characterized by high *NO* concentrations (~~mixing ratios (like a plume from~~ lightning emissions) which is transported both during the day and night.



Furthermore, the nitrate radical can potentially reacts with VOCs. The reaction of the unsaturated hydrocarbons such as, isoprene, butenes, and monoterpenes, with *NO*<sub>3</sub> leads to the *HNO*<sub>3</sub> formation (Monks, 2005) (reaction *R11*).



Considering *NO*<sub>3</sub> reaction with alkenes, an additional mechanism is found initiating a complex chemistry allowing to form *NO*<sub>2</sub> or organic nitrates (Monks, 2005). Finally, *NO*<sub>3</sub> can initiate the VOCs oxidation via peroxy radical production (reaction *R12*). That way, it can involve as a chain propagator (reactions *R13* to *R17*).



365



The reactions of *HO*<sub>2</sub> with ozone (*R16*) or *NO*<sub>3</sub> (*R17*) imply *OH* production. Also, the reaction of ozone with alkenes ~~allows to form~~ allowing formation of *OH* during the night (reaction *R18*) (Aumont, 2005).

375



The reaction *R18* occurs when ozone concentrations remain sufficiently high in night conditions, in other words for polluted atmosphere.

380 In this context, we consider different values at daytime and nighttime for the plume lifetime, the effective reaction rate constant and for the fraction of  $NO_x$  conversion into  $HNO_3$  within the plume. Distinguishing day and night chemistry is linked with the fluctuation of the critical  $r_l$  value (below which the sub-grid plume chemistry is negligible) depending on atmospheric conditions. Therefore, if  $r_l$  changes with sunlight, the plume lifetime changes also. Note that except the  $\beta_2$  fraction, this  
385 night chemistry is not considered by the initial plume approach developed by Cariolle et al. (2009), which considers  $NO_x$  plumes from aircraft exhausts only at daytime.

Figure 1 summarizes all elements which define the plume approach and how it has been adapted and implemented into the model.

### 390 3.2 Parameter calculations for lightning $NO_x$ emissions

In order to reproduce more accurately the lightning  $NO_x$  sub-grid chemistry, some points should be considered: (i) the latitude ( $NO_x$  emissions by lightning are higher in tropics than in mid-latitudes); (ii) the sunlight conditions (day and night) which impacts photochemistry and heterogeneous chemistry; (iii) the plume evolution with its own physical characteristics (the lifetime and the dispersion  
395 properties); and finally (iv) chemical interactions within the plume related to ~~high concentrated~~ fraction of highly elevated  $NO_x$  ~~considerably higher than background concentrations~~ concentrations relative to the background. In the following section, physical and chemical characteristics of the plume associated with lightning  $NO_x$  source have been defined.

#### 3.2.1 Dynamical conditions

400 The horizontal diffusion coefficient ( $D_h$ ) is a key parameter of the atmospheric dynamical conditions in determining the dispersion of the lightning  $NO_x$  plume.  $D_h$  is used as the dispersion constraint for the simple plume dispersion simulations carried out in order to estimate the plume lifetime and the effective reaction rate constant. The diffusion coefficient was ~~defined by~~ determined by two different ways. A first estimate of the horizontal diffusion was performed by running the 3-D  
405 mesoscale Meso-NH model ~~but mainly from previous~~. Then, the  $D_h$  coefficient was calculated using in-situ measurement measurements in thunderstorm anvil.

The Meso-NH mesoscale model was used (see section 2.2) to investigate  $D_h$ . A simple convective cell forced by warm bubble and initialized by a radiosounding at the ~~beginning of the simulation~~  
410 simulation start was run as an ideal case. Simulations were realized for a domain of 24 km in the two horizontal directions and the grid horizontal resolution is  $\Delta x = \Delta y = 1$  km and  $\Delta z = 500$  m. The convective cell is located at  $43.29^\circ N$  latitude and  $0^\circ$  longitude (Klemp and Wilhelmson, 1978). Simulations of 6 hours were ~~made~~ performed allowing the complete development and the dissipation of the convective cell.  $D_h$  has been calculated within the anvil using the mixing length diagnostic

415 variable, hereafter denoted  $L$ , as described by the equation 16 (Cuxart et al., 1999).

$$D_h = \frac{2}{3} \times \frac{L}{4} \times \underline{e^{\frac{1}{2}} \exp(\frac{1}{2})} \quad (16)$$

At the mature stage of the cell,  $D_h$  was calculated as  $100 \text{ m}^2 \cdot \text{s}^{-1}$  within the upper levels of the convective cell (i.e. in the anvil, defined empirically).

420 In addition to modeling estimate, we used in-situ measurements to calculate  $D_h$ . Turbulence measurements were performed by a B-757 commercial aircraft along a ~~flight~~flight from the west of Kansas to the north of Missouri and corresponding to a trajectory of more than 500 km (Trier and Sharman, 2008). These in-situ measurements were accomplished from 0700 to 1000 UTC the 17 June, 2005, during the development of a mesoscale convective system (MCS). This MCS is associ-  
425 ated with a turbulence event characterized by the measurement of the atmospheric eddy dissipation rate ( $\epsilon$ ) and the turbulence kinetic energy ( $TKE$ ) above and within the cloud anvil. The higher values of  $\epsilon$  ( $\epsilon^{1/3} \sim 0,4 \text{ m}^{2/3} \cdot \text{s}^{-1}$ ) were recorded between 11.3 and 11.6 km altitude corresponding to the cloud anvil levels. In addition, for this MCS, the TKE was about  $1 \text{ m}^2 \cdot \text{s}^{-2}$  at the locations of the highest  $\epsilon$  values.

430

According to these observations, the turbulent diffusivity (equation 17) was estimated above the anvil of the MCS ([http://www.ral.ucar.edu/projects/turb\\_char/](http://www.ral.ucar.edu/projects/turb_char/)) such as:  $D_h > 0.1 \text{ m}^2 \cdot \text{s}^{-2}$ . Then,  $D_h$  was calculated within the anvil such as:  $D_h = 15 \text{ m}^2 \cdot \text{s}^{-1}$  using the same formulation (equation 17). This last estimate seems to be the most common value compared to the diffusion coefficient  
435 value of  $20 \text{ m}^2 \cdot \text{s}^{-1}$  used by Cariolle et al. (2009), close to the tropopause level and the  $D_h$  value calculated for contrails ( $15 \text{ m}^2 \cdot \text{s}^{-1}$ ) in the upper troposphere (Knollenberg, 1972).

$$D_h = \frac{(TKE)^2}{\epsilon} \quad (17)$$

The  $D_h$  estimate using Meso-NH model is high compared to the results from measurements and corresponds to the upper limit of the calculated diffusion coefficients and could be associated with  
440 the turbulence in the convective cloud. However, it is important to note that usually most numerical simulations are performed with 1-D turbulence models. What is interesting in the use of Meso-NH in this study is that the 3-D turbulence is solved. This simulation provides an additional estimate of  $D_h$  allowing comparison with the calculation from in-situ measurements. Moreover, studies on the diffusivity in cloud anvils are uncommon. It is necessary to conduct additional work in the future  
445 on that issue again constrained with new in-situ measurements of the atmospheric turbulence in the anvil.

It is important to note that the 3-D turbulence is not solved online in the GEOS-Chem model because of the fine scale characterizing this process but prescribed by the GEOS-5 met fields.

450 Therefore, the global variability of  $D_h$  is not calculated by the CTM and it is beyond the scope of this study.

In order to cover all horizontal diffusivity estimates discussed in this section the range of values 0.1, 15 and  $100 \text{ m}^2 \cdot \text{s}^{-1}$  was used. The horizontal coefficient is constant for all lightning  $\text{NO}_x$  plumes which are considered in the GEOS-Chem model. Hereafter, the results are detailed for the central value  $D_h = 15 \text{ m}^2 \cdot \text{s}^{-1}$ . Sensitivity tests depending on the uncertainty associated with the parameter estimate are performed and presented later in section 4.3.

### 3.2.2 The $\text{NO}_x$ critical plume content ( $r_l$ )

The  $r_l$  critical value is the  $\text{NO}_x$  concentration-mixing ratio within the undiluted phase of the plume below which the non-linear chemistry can be neglected (section 3.1). It has been estimated using the 0-D DSMACC chemical box model (section 2.2). Initial conditions for simulations carried out with the DSMACC box model are from outputs of the GEOS-Chem model. Especially, initial atmospheric parameters and atmospheric background concentrations of species correspond to the average of the GEOS-Chem outputs (i) from 8 km to 11 km, (ii) for two latitude regions (tropics and mid-latitudes), and (iii) for the year 2006 (table 1). The altitude range refers to the detrainment region estimated by GEOS-Chem using the GEOS-5 met fields (section 2.1) both in the tropics and in the mid-latitudes. Note that this range could vary depending on the met fields and the convection parameterization. In addition, the  $\text{LNO}_x$  plume parameterization should have an impact outside of this altitude range mainly between 6 km and 12 km but in a lesser extent.

470

In order to focus on chemistry interactions only between chemical species of interest and removing the mixing influence and sunlight fluctuations, short simulations (i.e. one hour each) were run with the DSMACC model. The effects of the day or night conditions were carefully considered carrying out separate simulations at daytime and nighttime. Simulations were run for a large range of initial  $\text{NO}$  concentrations-mixing ratios from 0.01 ppb to 1 ppm. The  $r_l$  value is defined from the  $\text{NO}$  value for which the  $\frac{\partial O_x}{\partial t}$  trend is perturbed. In other words,  $r_l$  is associated to the second derivative of  $O_x$ , i.e. the curve optimums on figure 2. The  $r_l$  threshold was defined as to be 0.1 and 0.25 ppb during the day and night for mid-latitudes and 0.1 and 0.75 ppb during the day and night in the tropics (figure 2).

480

Note that the mid-latitudes and the tropics were separated because of the large differences in  $\text{LNO}_x$  emissions between the two regions in terms of the number of flashes in a particular convective cell which is higher in the tropics according to the LIS/OTD climatologies (Christian et al., 2003). This last point is important for the plume lifetime estimate detailed in the following section.



### 485 3.2.3 The plume lifetime $\tau$

The plume lifetime ( $\tau$ ) depends directly on (i) the initial  $NO$  pulse from lightning emissions, (ii) the  $r_l$  critical value, and (iii) the diffusion properties of the atmosphere. The plume lifetime also depends on the initial size of the plume. Here we use a width of 500 m to refer to an ensemble of spikes at the cloud scale ~~(i.e. each plume is defined from several electrical discharges at a convective cell scale).~~

490  $\tau$  is crucial for the physical description of the  $NO_x$  plumes and it has been computed in carrying out dispersion simulations of a simple plume assumed to be cylindrical. ~~The simple model is composed of 30 levels of dispersion. In the~~ In this model, the standard atmospheric conditions are represented by temperature, pressure and species concentrations of the background atmosphere, which are similar to the initial conditions used for the DSMACC simulations. As a reminder, initial conditions are 495 from GEOS-Chem outputs averaged (i) from 8 km to 11 km, (ii) for two latitude regions (tropics and mid-latitudes), and (iii) for the year 2006 (table 1). Simulations are initialized by a  $NO$  pulse from lightning emissions (hereafter denoted  $NO_i$ ) and the plume dispersion depends on the  $D_h$  value estimated in section 3.2.1.

500 The initial tracer concentrations  $NO_i$  related to lightning  $NO$  emissions at the scale of a convective cell (gathering several flashes together) in mid-latitudes were defined according to previous aircraft measurement campaigns. Especially, the STERAO campaign recorded  $NO$  spikes of magnitude from 1-10 ppb related to lightning activity in thunderstorms occurring 9-10 July 1996 over ~~the~~ northern Colorado (Dye et al., 2000; Stith et al., 1999). Lange et al. (2001) measured  $NO$  spikes 505 of 3.5 ppb during the STREAM campaign associated with a matured storm over ~~the~~ Ontario. Several peaks of  $NO$  mixing ratios from 0.7-6 ppb were also observed during EULINOX (Huntrieser et al., 2002) over Germany in July 1998. The LINOX aircraft campaign recorded  $NO$  spikes from 0.75-1.25 ppb (Huntrieser et al., 1998) related to thunderstorm over Europe, the 30 July 1996. From these studies, the  $NO$  concentration associated with the electrical activity in thunderstorms occurring over ~~the~~ mid-latitudes was determined as  $NO_i^{mean, Midlats} = 3.4$  ppb ( $NO_i^{min, Midlats} = 0.7$  ppb and  $NO_i^{max, Midlats} = 10$  ppb). Because there are much fewer  $LNO_x$  measurements in the tropics and in order to be consistent with the  $LNO_x$  emissions defined in the GEOS-Chem model, the ratio  $R_{LNO_x} = \frac{LNO_x^{Midlatitudes}}{LNO_x^{Tropics}}$  was defined as in the CTM. During the year 2006, the relative mid-latitudes and tropics  $LNO_x$  contribution was about  $R_{LNO_x} = 0.33$ . This result is in agreement with 515 higher  $LNO_x$  emissions in these regions rather than in ~~the~~ mid-latitudes. The value of  $NO$  mixing ratio injected by lightning in ~~tropics was defined the tropics was estimated~~ as  $NO_i^{mean, Tropics} = 10.2$  ppb ( $NO_i^{min, Tropics} = 2.8$  ppb and  $NO_i^{max, Tropics} = 29.7$  ppb).

Once  $NO_i$  estimate was completed, the calculation of the plume lifetime was achieved using the 520 detailed formulation given in section 3.1.1. The results for  $\tau$  are summarized in table 2. Hereafter, the results are detailed for  $NO_i^{mean}$  in section 4 and sensitivity tests are carried out using all  $NO_i$  values

for ~~midlatitudes and the~~ mid-latitudes and the tropics (section 5). Model calculations for  $NO_i^{mean}$  and  $D_h = 15 \text{ m}^2 \cdot \text{s}^{-1}$  provide a minimum plume lifetime of 3 (6) hours for the mid-latitudes and maximum plume lifetime of 9 (21.3) hours for the tropics at daytime (nighttime).

### 525 3.2.4 The effective reaction rate constant ( $K_{eff}$ )

The non-linear chemistry within the plume has been considered in calculating the effective reaction rate constant ( $K_{eff}$ ), which is used to compute the formation of the secondary species ( $O_x$  and  $HNO_3$ ) within the plume. That corresponds to the evolution of odd oxygen depending on the  $O$  and  $O_3$  reactions with  $NO_2$  and  $NO$ , and also on the  $NO_x$  activation (day) or deactivation  
 530 (night) with the  $HNO_3$ ,  $N_2O_5$  and  $PAN$  chemistry. Note that in the case of lightning emissions other species like VOCs,  $HO_x$  and  $H_2O$  may be uplifted in the convective region. However, we assumed that the OPE is mainly controlled by  $NO_x$  in the upper troposphere as previously showed by Sauvage et al. (2007b). Therefore,  $K_{eff}$  calculation is here mainly dependent on  $NO_x$  content. Future studies should try to investigate this issue for lightning emissions mixed with strong surface  
 535 emissions in order to sharpen our parameterization.

$K_{eff}$  is calculated according to the equation 11 of the section 3.1.2 using the same simple plume dispersion simulations than those carried out to define the plume lifetime (section 3.2.3).

540 Results for  $K_{eff}$  are summarized in table 3. Model calculations using  $NO_i^{mean}$  and  $D_h = 15 \text{ m}^2 \cdot \text{s}^{-1}$  give a  $K_{eff}$  value of  $5.49 \cdot 10^{-19} \text{ molecules}^{-1} \cdot \text{s}^{-1} \cdot \text{cm}^3$  ( $4.55 \cdot 10^{-19} \text{ molecules}^{-1} \cdot \text{s}^{-1} \cdot \text{cm}^3$ ) in the mid-latitudes and  $3.64 \cdot 10^{-19} \text{ molecules}^{-1} \cdot \text{s}^{-1} \cdot \text{cm}^3$  ( $2.98 \cdot 10^{-19} \text{ molecules}^{-1} \cdot \text{s}^{-1} \cdot \text{cm}^3$ ) in the tropics, at daytime (at nighttime).

545 ~~Our  $K_{eff}$  estimations obtained in this study are very low as well as estimates are smaller than~~ those calculated by Cariolle et al. (2009) ~~;~~ for the plume chemistry related to aircraft exhausts. In this previous work,  $K_{eff}$  varies from  $1.0$  to  $4.2 \cdot 10^{-18} \text{ molecules}^{-1} \cdot \text{s}^{-1} \cdot \text{cm}^3$  with a mean value close to  $3 \cdot 10^{-18} \text{ molecules}^{-1} \cdot \text{s}^{-1} \cdot \text{cm}^3$  depending on the  $NO_x$  loading. The very low value for  $K_{eff}$  point out that the plume parameterization implies a delay of the production of ozone at the  
 550 large scale rather than its destruction within the plume.

### 3.2.5 The fractions of $NO_x$ conversion to $HNO_3$ ( $\beta_1$ and $\beta_2$ )

The fractions  $\beta_1$  and  $\beta_2$  represent the  $NO_x$  conversion into  $HNO_3$  within the plume at daytime and nighttime respectively. They were computed using the DSMACC chemical box model.

555 The  $\beta_1$  coefficient was calculated for day conditions depending mainly on the  $OH$  concentration. The conversion of  $NO_x$  into  $HNO_3$  at nighttime ( $\beta_2$  coefficient) is related to the heterogeneous

reaction of  $N_2O_5$  and so depends on particles (aerosols and ice crystals) concentration and their lifetime. This is directly linked with the surface density and the radius of particles in the anvil region of thunderstorms, which is highly uncertain. We defined these values using in situ measurements. The surface area ( $S_T$ ) and the radius ( $R$ ) for aerosols are defined such as:  $S_T = 0.28 \text{ m}^{-1}$  and  $R = 1 \text{ }\mu\text{m}^{-1}$  (Huntrieser et al., 2002) and for ice,  $S_T = 0.03 \text{ m}^{-1}$  and  $R = 30 \text{ }\mu\text{m}^{-1}$  (Knollenberg et al., 1993). In addition, the reaction probabilities of  $NO_x$  on aerosols and ice crystals  $\gamma_{N_2O_5}^{aerosols} = 0.02$  (Evans and Jacob, 2005) and  $\gamma_{N_2O_5}^{ice} = 0.03$  (Sander et al., 2006), respectively, were used for our box model simulations. These values correspond to the probability that a  $N_2O_5$  molecule impacting an aerosol or an ice crystal surface was subjected to react. The results for  $\beta_1$  and  $\beta_2$  coefficients are summarized in table 4.

The estimate of  $\beta_1$  fraction does not show significant variation neither between latitudes regions nor depending on  $NO_i$ . The minimum  $\beta_1$  value is  $1.34 \cdot 10^{-4}$  for the tropical regions and  $NO_i^{min}$ , and the maximum  $\beta_1$  value is  $1.88 \cdot 10^{-4}$  for the mid-latitudes and  $NO_i^{max}$ . The study of production and destruction rates for day conditions taking into account all reactions pathways (not shown here) demonstrates that production of  $HNO_3$  during the day is mainly determined by reaction of  $NO_3$  with formaldehyde ( $HCHO$ ) and acetaldehyde ( $CH_3CHO$ ). Surprisingly, the  $HNO_3$  formation via the  $NO_2 + OH$  reaction seems to be less efficient. This result could be explained by the low initial concentrations of  $OH$  used for the DSMACC simulations and it is in agreement with the small  $\beta_1$  values. Then, the averaged  $\beta_2$  coefficient is higher by a factor 10 compared to  $\beta_1$  with a minimum value of  $0.24 \cdot 10^{-3}$  in the tropics for  $NO_i^{max}$  and a maximum estimate of  $14.4 \cdot 10^{-3}$  in the mid-latitudes for  $NO_i^{min}$ . The analysis of the production and the destruction rates for night conditions taking into account all reactions pathway shows that the predominant reaction in the  $HNO_3$  evolution is  $N_2O_5 + H_2O$  (or the heterogeneous reaction on the aerosols and ice crystals surface).

## 4 Results: CTM simulations

In this section, the effects of the lightning  $NO_x$  plume parameterization, i.e. the influence of the sub-grid processes related to lightning emissions, on the  $NO_x$  and  $O_3$  tropospheric distributions at large scale are evaluated. Then, the parameterization sensitivity to initial  $NO$  mixing ratio injected by lightning ( $NO_i$ ),  $D_h$ ,  $\beta_1$  and  $\beta_2$  coefficients is analyzed to quantify the variability of the results regarding the plume-in-grid parameter calculations.

### 4.1 Implementation of the $LNO_x$ plume parameterization

The implementation of the lightning  $NO_x$  plume parameterization into the GEOS-Chem model requires specifying the system of continuity equations related to the plume chemistry solved at large

scale by the model (section 3.1.2, equations 13, 14 and 15). Lightning  $NO_x$  emissions calculated in each grid box (in  $molecules \cdot cm^{-2} \cdot s^{-1}$ ) by the model are directly used to compute the injection rate  $I$  ( $s^{-1}$ ) of  $NO$  at each chemical time step of the simulation. Then, we consider ~~the following setup: that~~  $\alpha_{NO_x} = 1$  ~~and  $E_{INO_x} = 1$ ,~~ in order to represent the mixing ratio of the undiluted fraction of  $NO_x$  by the tracer ( $r_{LNO_x}$ ). Furthermore, lightning produce ~~only negligible quantities of  $NO_2$  relative to  $NO$  among  $NO_x$  species thus  $E = 0$  and therefore  $E$  is 0~~ in the equation 15. Finally, the ratio  $\frac{NO_2}{NO_x}$  is the relative balance between  $NO$  and  $NO_2$  in the diluted phase at large scale reproduced by the model.

## 4.2 Impact of $LNO_x$ emissions on the $NO_x$ and $O_3$ distributions

We perform a spin-up of six months (from July 2005 to January 2006) in order to obtain a steady state in the model after activation of the plume parameterization. Then, simulations were run for the entire year 2006. The transport and the convection time steps are 15 minutes and the emissions and the chemical time steps are 30 minutes.

In the following, standard simulation refers to simulation with standard lightning  $NO_x$  emissions i.e. instantaneously diluted in a grid cell, while modified simulation refers to simulation considering the plume parameterization and then sub-grid chemistry. Note that the modified simulation was run using mean values for the initial  $NO$  mixing ratio ( $NO_i^{mean, Midlats} = 3.4$  ppb et  $NO_i^{mean, Tropics} = 10.2$  ppb) and  $D_h = 15$   $m^2 \cdot s^{-1}$ . The Base Case (BC) experiment corresponds to the standard simulation minus the standard simulation without lightning  $NO_x$  emissions. The  $P1$  experiment corresponds to the modified simulation minus the standard simulation without lightning  $NO_x$  emissions. The  $P2$  experiment is the same as the  $P1$  experiment but without considering the nitrification mechanism in the modified simulation (i.e.  $\beta_1 = \beta_2 = 0$ ). In addition, sensitivity tests were performed for  $P1$  defined by the modified simulation using the minimum and the maximum values for  $D_h$ ,  $NO_i$ ,  $\beta_1$  and  $\beta_2$  coefficients. All experiments are summarized in table 5.

Lightning emissions rates and the associated  $LNO_x$  tracer distributions are first discussed, then the effects of the implementation of the plume parameterization ( $P1$ ) compared to the experiment without the plume-in-grid development (BC case) is presented.

### 4.2.1 Lightning emissions and $LNO_x$ tracer distributions

Figure 3 displays the geographical distributions of the 9 km lightning  $NO_x$  emissions (a), the related  $LNO_x$  tracer distributions (b) and the  $LNO_x$  tracer zonal averaged (c) in January (top panels) and in July (bottom panels) reproduced by the CTM from the  $P1$  experiment. These results are shown for an approximate detrainment level (9 km altitude) where the ~~detrainment of  $LNO_x$  are the most concentrated~~ is the largest. In January, the highest emissions of  $NO_x$  from

lightning ( $4 - 6 \cdot 10^9 \text{ molecules} \cdot \text{cm}^{-2} \cdot \text{s}^{-1}$ ) are located in the southern hemisphere around the tropics over West Australia and Central-South Africa. Also, the model gives low  $LNO_x$  emissions ( $< 3 \cdot 10^9 \text{ molecules} \cdot \text{cm}^{-2} \cdot \text{s}^{-1}$ ) over South America and North America especially over the Gulf of Mexico. In July, the highest  $LNO_x$  emissions ( $4 - 6 \cdot 10^9 \text{ molecules} \cdot \text{cm}^{-2} \cdot \text{s}^{-1}$ ) are calculated in the northern hemisphere over North America, North of India, Central Africa and Sahel. In addition,  $LNO_x$  emissions are modeled over Europe and over East Asia but to a lesser extent ( $< 2 \cdot 10^9 \text{ molecules} \cdot \text{cm}^{-2} \cdot \text{s}^{-1}$ ).

The lightning  $NO_x$  tracer introduced into the model represents the lightning  $NO_x$  emissions affected by the transport and the exponential decay depending on the plume lifetime. Figure 3 shows that the tracer distribution is consistent with the lightning  $NO_x$  emissions. However, it is important to note that the plume lifetime is a key factor in the evolution of the  $LNO_x$  tracer mixing ratio. A long plume lifetime (several hours to several days) allows the intercontinental transport of  $LNO_x$  plumes. The representation of the sub-grid chemistry and the transport of the non-linear chemistry effects related to the plume consideration becomes important for the chemistry of the regions located far downwind from source regions. The plume lifetime depends on the latitude because of the different background chemical concentrations and the different amount of  $NO_x$  emitted from lightning in the tropics and in the mid-latitudes. In addition, as mentioned before, we consider the influence of day and night conditions on the plume lifetime estimate. According to its preliminary calculation (section 3.2.3), the plume lifetime is longer in the tropics (9 and 21.3 hours for day and night conditions, respectively) than in the mid-latitudes (3 and 6 hours, for day and night conditions, respectively). So, the  $LNO_x$  tracer is characterized by a shorter lifetime as a plume over North America than over Central Africa and around the Sahel while the model simulated ~~less important~~ fewer emissions over these regions especially in summer. In boreal winter, the mixing ratio of the lightning  $NO_x$  tracer calculated by the model is about 0.21 ppb over Central and South Africa, 0.18 ppb over West Australia and 0.11 ppb over South America. In summer, the tracer mixing ratio is simulated as 0.21 ppb, 0.32 ppb and 0.16 ppb over Central Africa, North India and North America, respectively. The lightning  $NO_x$  tracer is ~~mainly reproduced~~ produced at altitudes where lightning  $NO_x$  are ~~produced~~ calculated and detrained (in the upper troposphere between  $\sim 500$  and  $300$  hPa) as shown in panels (c) in figure 3.

#### 4.2.2 Impact of lightning on $NO_x$ and $O_3$ distributions with the plume parameterization

The difference between  $P1$  and  $BC$  experiments ( ~~$P1 - BC$~~ ) ( $P3$ ) was calculated in order to quantify the changes on  $NO_x$  and  $O_3$  mixing ratios at large scale implied by the implementation of the plume-in-grid parameterization into GEOS-Chem. Figures 4 and 5 display the geographical distributions of the  $NO_x$ ,  $HNO_3$ ,  $PAN$  and  $O_3$  absolute changes (in ppb) in January and in July, respectively. The 9 km altitude level was chosen because of the most significant variations at this

altitude compared to the rest of the troposphere.

In boreal winter,  $LNO_x$  plume chemistry leads to a maximum decrease at large scale over regions of emissions of 120 ppt for  $NO_x$  and a decrease of 68 ppt for  $HNO_3$  and 16 ppt for  $PAN$  over Central and South Africa. These variations are associated with a maximum  $O_3$  decrease of 2.8 ppb over regions of emissions. A similar  $NO_x$ ,  $HNO_3$ ,  $PAN$  and  $O_3$  reduction is obtained in other areas of high  $LNO_x$  emissions (i.e. over West Australia and South America). Downwind of  $LNO_x$  emissions, the opposite effect is observed for  $NO_x$  and  $HNO_3$  species with maximum increase of 40 ppt for  $NO_x$  and 13.5 ppt for  $HNO_3$  observed over South Atlantic and Indian Ocean. Generally,  $PAN$  still decreases over oceans but in a lesser extent compared to regions of  $LNO_x$  emissions, with a maximum reduction of 9 ppt.  $O_3$  response is a maximum increase of 1.13 ppb around area where the transport is effective and especially over the oceans. In summer, maximum decreases of 140 ppt for  $NO_x$  and 60 ppt for  $HNO_3$  and 24 ppt for  $PAN$  are calculated by the CTM leading to a maximum  $O_3$  decrease of 2.4 ppb over Central Africa (reduction also observed over North America and North India). Downwind of lightning emissions, increase of  $NO_x$  and  $HNO_3$  is observed with a maximum value of 30 ppt and 38 ppt, respectively.  $PAN$  reservoir species also still decreases slightly downwind with 2 ppt changes. Finally, that leads to maximum  $O_3$  increase of 0.7 ppb.

Note that the production of  $PAN$  is limited by the supply of  $NO_x$  or non-methane ~~volatile~~ volatile organic compounds (NMVOCs). Above continental lightning sources regions, NMVOCs are uplifted by deep convection but with lower  $NO_x$  due to the activation of the plume parameterization. That implies a less efficient  $PAN$  production in these regions. Downwind of lightning sources regions (oceanic regions),  $NO_x$  increases because of the  $LNO_x$  transport in the plume form but there is less NMVOCs available to produce  $PAN$ . Therefore, ~~the both in regions of  $LNO_x$  emissions and downwind, the  $PAN$  production is limited leading to an overall lower  $PAN$  production-mixing ratios at large scale in P1 experiment. However, this may be nuanced by considering the  $PAN$  chemistry in future studies using similar  $LNO_x$  plume parameterization by introducing the  $PAN$  and  $CH_3C(O)OO$  continuity equations and a new term to consider the fraction of  $NO_x$  converted to  $PAN$  within the plume. This should allow the  $PAN$  production during the plume transport, which is inhibited in the current version.~~

In order to provide a full overview of the effects of the plume parameterization, the relative difference between the  $P1$  and  $BC$  experiments (i.e.  $(P1 - BC) / BC$ ) was calculated integrated throughout the troposphere. Figures 6 and 7 show zonal averaged of  $NO_x$  (upper panels) and  $O_3$  (bottom panels) relative changes (in %) integrated throughout the troposphere for regions of interest for January and July, respectively. During boreal winter, the highest  $NO_x$  ( $O_3$ ) decreases of 10 % (5 %) in West Australia, then 20 % (6 %) in Central Africa are calculated. These negative variations

are mainly calculated between 400 hPa and the tropopause level for  $NO_x$  and ozone. South America  
 700 is characterized by a decrease of 20 % of the nitrogen oxides and 1 % of ozone. Over this region,  
 variations are significant in the entire troposphere for both species. In contrast to the continent de-  
 crease,  $NO_x$  increase is observed over the major part of South Atlantic and Indian Ocean with 14 %  
 and 20 % maximum, respectively. The  $O_3$  response is an increase of 1 % near the tropopause and it  
 becomes higher close to the surface of about 4 %. In summer, there is a  $NO_x$  ( $O_3$ ) decrease of 25 %  
 705 (8 %) over Central Africa, 20 % (2 %) over North India, and 5 % (0.5 %) over North America. Also,  
 South Atlantic and Indian Ocean (located downwind of lightning  $NO_x$  emissions) are characterized  
 by a maximum increase of 18 % for  $NO_x$  and 2 % for  $O_3$ .

As a result, the sub-grid chemistry associated to the  $LNO_x$  emissions implies (i) a decrease of  
 710 the nitrogen oxides and ozone mixing ratios at large scale over regions characterized by intense  
 lightning emissions and (ii) an increase of these species downwind of emissions. Especially the  
 plume parameterization related to the lightning  $NO_x$  leads to:

1. Significant effects on  $NO_x$  mixing ratio ( $\pm 20$  %): these effects on nitrogen oxides are impor-  
 tant because  $NO_x$  is the first criterion which is constrained in a CTM in order to determine  
 715 the global  $LNO_x$  production ( $6 \text{ TgN} \cdot \text{yr}^{-1}$  in the GEOS-Chem model);
2. Lower effects on  $O_3$  mixing ratio ( $\pm 5$  %): these limited impacts on ozone could be explained  
 by compensatory effect of the  $NO_y$  species (mainly conversion of  $NO_x$  into  $HNO_3$  within  
 the plume ~~or (ii) PAN~~).

The effects of the plume parameterization are simulated over the entire troposphere mainly for ozone.  
 720 Indeed, the spreading of effects on ozone to the lower free troposphere is related to the subsidence  
 areas of the Walker circulation. These regions are characterized by the accumulation and creation  
 of ozone for low altitude levels. Nevertheless, the maximum  $NO_x$  and  $O_3$  variations are calculated  
 for altitude levels associated with a mean detrainment level. The more realistic representation of the  
 sub-grid processes ( $P1$  experiment) related to the  $LNO_x$  plume is in contrast with the simplified  
 725 instantaneous dilution in the grid cell of the lightning  $NO_x$  emissions (BC experiment).

The plume approach allows the conversion of  $NO_x$  into  $HNO_3$  during the plume lifetime. In  
 addition, the high  $NO_x$  concentration within the plume (much higher than the background content)  
 leads to the  $O_3$  titration and more generally to the  $O_x$  destruction within the plume. The most im-  
 730 portant impact of the plume parameterization is the transport of the  $LNO_x$  emissions as a plume  
 and the transport of the associated non-linear chemistry effects leading to a delay of the  $O_3$  produc-  
 tion at large scale. In other words,  $O_3$  is less produced over the regions with intense lightning  $NO_x$   
 emissions than downwind of  $LNO_x$  emissions by photochemical reactions from  $NO_x$ .



### 4.3 Plume sensitivity to the estimated uncertainties of parameter calculations

#### 4.3.1 The Atmospheric dynamical conditions and the initial $NO$ mixing ratio injected by lightning

The impact of (i) the diffusion properties of the atmosphere ( $D_h$ ) and (ii) the initial  $NO$  mixing ratio injected by lightning ( $NO_i$ ) are analyzed.  $D_h$  and  $NO_i$  are the two key parameters in the determination of the physical and chemical characteristics of the plume. The modified simulation characterizing the  $P1$  experiment was run for the ranges of the horizontal diffusion coefficients and the initial  $NO$  mixing ratio injected by lightning. It is important to note that for these sensitivity tests,  $\beta_1$  and  $\beta_2$  coefficients remain constant using their mean values.  $\tau$  and  $K_{eff}$  values related to these simulations are those previously calculated (section 3) and summarized in tables 2 and 3. Figure 8 displays  $\tau$  (upper panels) and  $K_{eff}$  (bottom panels) variations depending on  $D_h$  and  $NO_i$ . As expected, the strongest the horizontal diffusion is the most efficient the dispersion of the plume is. In both, the mid-latitudes and the tropics,  $\tau$  decreases when  $D_h$  becomes larger. In addition,  $\tau$  increases with the initial  $NO$  mixing ratio injected by lightning. In contrary,  $K_{eff}$  increases with  $D_h$  coefficient in the two regions of the globe.

The ~~variability of~~ sensitivity of the  $NO_x$  and  $O_3$  mixing ratios around the mean value for regions and seasons depending on the known uncertainties associated with parameter calculations have been quantified. Figure 9 shows the ~~intervals of variability~~ ranges of sensitivity of  $NO_x$  and  $O_3$  ( $\Delta NO_x$  and  $\Delta O_3$ , respectively) at 9 km altitude reproduced by GEOS-Chem depending on  $D_h$  and on the initial  $NO$  mixing ratio ( $NO_i$ ). Note that for the sake of readability, the scale of  $NO_x$  and  $O_3$  changes differs by region. Results are also summarized in table 6.

We chose representative continental areas such as Florida and Congo, which correspond to regions characterized by intense electrical activity for the mid-latitudes and the tropics, respectively. North and South Atlantic were selected to represent regions downwind of  $NO_x$  emissions, for ~~mid-latitude and tropic~~ the mid-latitudes and the tropics variations, respectively. The highest ~~ranges of~~  $NO_x$  and  $O_3$  ~~changes~~ ranges are obtained for continental tropical regions with  $\Delta NO_x$   $[-33.1; +29.7]$  ppt and  $\Delta O_3$   $[-1.56; +2.16]$  ppb, in January, and  $\Delta NO_x$   $[-14.3; +21]$  ppt and  $\Delta O_3$   $[-1.18; +1.93]$  ppb, in July. The largest ~~variation~~ range associated with the tropical continents could be explained by the largest difference on parameter values defining the plume in this region (especially  $NO_i$ ). The smallest ~~intervals~~ changes are observed over continental mid-latitude regions for winter with  $\Delta NO_x$   $[-1.7; +1.8]$  ppt and  $\Delta O_3$   $[-0.16; +0.72]$  ppb and over oceanic tropical regions in summer such as  $\Delta NO_x$   $[-11.5; +2.6]$  ppt and  $\Delta O_3$   $[-0.14; +0.92]$  ppb. As a result, the ~~variability~~ sensitivity of  $NO_x$  and  $O_3$  species to the parameter uncertainties is a few ppt for  $NO_x$  and less than 2 ppb for  $O_3$ .



### 770 4.3.2 Coefficients related to the nitrification mechanism ( $\beta_1$ and $\beta_2$ )

In order to estimate the ~~variability-sensitivity~~ of the  $NO_x$  and  $O_3$  mixing ratios related to the uncertainties on  $\beta_1$  and  $\beta_2$  fractions (table 7), the difference between  $P1$  experiment using  $\beta_1$  and  $\beta_2$  mean values and  $P1$  experiment using minimum and maximum  $\beta_1$  and  $\beta_2$  coefficients has been calculated. This implies that  $\tau$  and  $K_{eff}$  are constant.

775

In January, the highest ~~variability-sensitivity~~ on  $NO_x$  mixing ratio is  $\Delta NO_x [-2.3; +0.9] \cdot 10^{-2}$  ppt over ~~the~~ continental tropical regions and  $\Delta O_3 [-10; +11] \cdot 10^{-4}$  ppb over ~~the~~ tropical ocean on  $O_3$ , while ~~mid-latitude-the mid-latitudes~~ oceanic areas show minimum ranges on  $NO_x$  and  $O_3$  with  $\Delta NO_x \pm 2.3 \cdot 10^{-2}$  ppt associated with  $\Delta O_3 [-9; +4] \cdot 10^{-4}$  ppb. In July, the maximum ranges are  
 780 calculated over oceans in ~~the~~ mid-latitudes for  $NO_x$  such as  $\Delta NO_x [-21.1; +6.6] \cdot 10^{-2}$  ppt and in ~~the~~ tropics for  $O_3$  with  $\Delta O_3 [-30; -2] \cdot 10^{-4}$  ppb. Finally, the smallest ~~intervalschanges~~,  $\Delta NO_x [-0.9; -0.4] \cdot 10^{-2}$  ppt and  $\Delta O_3 [-24; -6] \cdot 10^{-4}$  ppb, are simulated for ~~the~~ tropical ocean and ~~mid-latitude-the mid-latitudes~~ continent, respectively.

785 In addition, the impact of the nitrification mechanism was assessed comparing the  $P1$  experiment using mean  $\beta_1$  and  $\beta_2$  values and  $P2$  experiment for which  $\beta_1 = \beta_2 = 0$ . As a result, taking into account  $NO_x$  conversion into  $HNO_3$  using the mean  $\beta$  fractions calculated in this study does not imply strong changes in  $NO_x$  and  $O_3$  distributions ( $\Delta NO_x < 10^{-4}$  ppb and  $\Delta O_3 < 10^{-2}$  ppb).

790 In the case of significant values of  $\beta$  fractions, the rate of the nitrification mechanism should imply a delay of the  $O_3$  formation from the  $NO_x$  in the plume because of the  $NO_x$  storage ~~into-in~~  $HNO_3$ . On the other hand,  $HNO_3$  is considered as a one of the main sink for  $NO_x$  species undergoing wet deposition and seemingly limiting their affect on global ozone.

795 The sensitivity tests point out the limited effect of the  $NO_x$  conversion to  $HNO_3$  within the plume using our  $\beta_1$  and  $\beta_2$  ~~estimates. The variability-calculations. The sensitivity~~ on  $NO_x$  and  $O_3$  mixing ratios related to  $\beta$  coefficients is about a few ppt. ~~That could be explained by small- $\beta$  values resulting from our estimate unlike Cariolle et al. (2009) highlighted the significant influence of these fractions-Indeed, our  $\beta_1$  and  $\beta_2$  estimates are smaller than those calculated by Cariolle et~~  
 800 ~~al., 2009 ( $\beta_1 = 0.06$  and  $\beta_2 = 0.2$ ), which showed a large impact of this mechanism~~ in the case of aircraft  $NO_x$  emissions. ~~In-our~~ ~~In the present~~ study, we can easily suppose that the increase of the  $\beta_1$  and  $\beta_2$  coefficients should be in agreement with the work of Cooper et al. (2014) in reducing the ~~underestimation-of-underestimate of the~~  $HNO_3$  production induced by  $NO_x$  emissions from lightning. Further estimates of  $\beta$  should be realized using future observations in cloud anvil of primary  
 805 species, aerosols and particules needed for  $NO_x$  conversion at daytime and nighttime to improve the determination of these parameters. ~~The~~  $\beta_1$  coefficient is particularly dependent on the  $HO_x$  radicals,

which could vary significantly within the cloud anvil in part because of the transport of peroxides from the lower troposphere by convective uplift (Wennberg et al., 1998). Then, the determination of  $\beta_2$ , corresponding to the  $NO_x$  conversion fraction into  $HNO_3$  via  $N_2O_5$  formation during night-  
810 time is considerably dependent on (i) the estimate of aerosols and the ice crystal concentration and their lifetime within the cloud anvil which is highly uncertain according to measurement campaigns and (ii) on the reaction probability on aerosols  $\gamma_{N_2O_5}^{aerosol}$  and ice crystals  $\gamma_{N_2O_5}^{ice}$  from laboratory studies extrapolations.

815 According to results presented in this section, the sensitivity tests show the predominance of the initial  $NO$  mixing ratio injected by lightning ( $NO_i$ ) and the diffusion properties of the atmosphere ( $D_h$ ) in the variability of the  $NO_x$  and  $O_3$  mixing ratios around the mean value in response to the plume-in-grid parameterization in the CTM. In winter, the  $NO_x$  and  $O_3$  ~~variability-sensitivity~~ is the highest for continental regions in the tropics and the smallest ~~variability-sensitivity~~ is calculated for  
820 the mid-latitudes. In summer, the most important ~~variability-sensitivity~~ of  $NO_x$  and  $O_3$  is simulated in the tropics over regions characterized by intense  $LNO_x$  emissions while the least significant sensitivity is obtained still in the tropics but downwind of emissions (mainly over oceans).

## 5 Conclusions

For the first time, a more realistic lightning  $NO_x$  chemistry is implemented as a plume parameteriza-  
825 tion into a global chemical transport model. The key parameters characterizing the lightning-related plume were estimated depending on two main criteria, i.e. the  $NO$  mixing ratio injected by lightning ( $NO_i$ ) and the atmospheric diffusion coefficient ( $D_h$ ).

According to the  $NO_i$  and  $D_h$  ranges, the plume lifetime ( $\tau$ ) and the effective reaction rate con-  
830 stant ( $K_{eff}$ ) for  $NO_x$ - $O_3$  chemical interactions were estimated as follow:

- $\tau = [0.01; 68.5]$  hours;
- $K_{eff} = [0.77; 23] \cdot 10^{-19} \text{ molecules}^{-1} \cdot \text{s}^{-1} \cdot \text{cm}^3$ .

Also, for the conditions defined by  $NO_i^{mean}$  and  $D_h = 15 \text{ m}^2 \cdot \text{s}^{-1}$ :

- $\tau$  is 3 (6) hours in the mid-latitudes and 9 (21.3) hours in the tropics at daytime (nighttime);
- 835 –  $K_{eff}$  is  $5.49 \cdot 10^{-19} \text{ molecules}^{-1} \cdot \text{s}^{-1} \cdot \text{cm}^3$  ( $4.55 \cdot 10^{-19} \text{ molecules}^{-1} \cdot \text{s}^{-1} \cdot \text{cm}^3$ ) in mid-latitudes and  $3.64 \cdot 10^{-19} \text{ molecules}^{-1} \cdot \text{s}^{-1} \cdot \text{cm}^3$  ( $2.98 \cdot 10^{-19} \text{ molecules}^{-1} \cdot \text{s}^{-1} \cdot \text{cm}^3$ ) in the tropics at daytime (nighttime).

Finally, the fractions of  $NO_x$  conversion into  $HNO_3$  within the plume are  $\beta_1 = [1.34; 1.88] \cdot 10^{-4}$ , and  $\beta_2 = [0.24; 14.4] \cdot 10^{-3}$  for day and night conditions respectively.

GEOS-Chem simulations performed using mean value for  $NO_i$  and  $D_h = 15 \text{ m}^2 \cdot \text{s}^{-1}$  reveal nitrogen species and ozone changes compared to the instantaneous dilution. A decrease of  $NO_x$  and  $O_3$  mixing ratios at large scale over the regions of strong  $LNO_x$  emissions is observed mainly in the northern hemisphere in summer and in the southern hemisphere in winter. In the troposphere, maximum decrease of 20 % (6 %) in January and 25 % (8 %) in July for  $NO_x$  ( $O_3$ ), are found over Central Africa. In contrast, an increase of  $NO_x$  ( $O_3$ ) downwind of emissions is simulated of 20 % (4 %) in January and 18 % (2 %) in July. The  $LNO_x$  plume parameterization allows the transport of the effects on the non-linear chemistry occurring within the plume and the conversion of  $NO_x$  to the nitrogen reservoir species (mainly  $HNO_3$ ). However, the most significant impact is the transport of the  $LNO_x$  as a plume. That implies a delay of (i) the  $NO_x$  release into the point grid and (ii) ozone production from  $NO_x$  emitted by lightning flashes corresponding to the decrease of the  $NO_x$  and  $O_3$  mixing ratios at large scale over regions of emissions and their increase over transport pathway.

The ~~variability-sensitivity~~ of the  $NO_x$  and  $O_3$  mixing ratios around the mean value depending on the known uncertainties on the plume physics and chemistry key parameters has been estimated. The highest sensitivity is obtained for the continental tropical regions with  $\Delta NO_x$   $[-33.1; +29.7]$  ppt and  $\Delta O_3$   $[-1.56; +2.16]$  ppb, in January, and  $\Delta NO_x$   $[-14.3; +21]$  ppt and  $\Delta O_3$   $[-1.18; +1.93]$  ppb, in July. Concerning the  $\beta_1$  and  $\beta_2$  fractions, the highest ~~variability-sensitivity~~ depending on the fraction uncertainties for  $NO_x$  is  $\Delta NO_x$   $[-2.3; +0.9] \cdot 10^{-2}$  ppt over the continental tropical regions, and  $\Delta O_3$   $[-10; +11] \cdot 10^{-4}$  ppb for  $O_3$  over the tropical ocean in January. In summer, the maximum ranges are calculated over oceans in the mid-latitudes for  $NO_x$  such as  $\Delta NO_x$   $[-21.1; +6.6] \cdot 10^{-2}$  ppt and in the tropics for  $O_3$  with  $\Delta O_3$   $[-30; -2] \cdot 10^{-4}$  ppb. Accordingly, parameters leading to the highest uncertainties on results and which drive the plume-in-grid parameterization are  $NO_i$  and  $D_h$ .

This study demonstrates the importance to consider the plume-in-grid chemistry related to the lightning  $NO_x$  emissions occurring at smaller scale for global calculations. Taking into account the plume dilution into the background atmosphere in time and space with the transport of the  $NO_x$  and  $O_3$  non-linear chemistry effects and the conversion of  $NO_x$  into  $HNO_3$  reservoir species, implies more realistic  $NO_x$  and  $O_3$  concentrations in CTM. The plume-in-grid approach, by allowing a more realistic sub-grid chemistry will allow improving the different steps in the lightning  $NO_x$  emissions modeling such as the convection process, the calculation of the  $NO$  molecules produced by lightning discharges depending on regions according to recent and future satellite observations, and also processes like the  $HNO_3$  scavenging and the  $HNO_3$  uptake by ice crystals.

**Acknowledgements.** The GEOS-Chem community (Harvard University) and the Laboratoire d'Afologie (UPS / CNRS) supported this work. The authors acknowledge for the help of Lee T. Murray (NASA, NY, USA) for

his expertise on the lightning  $NO_x$  emissions module in the GEOS-Chem model. We thank the University Paul Sabatier III of Toulouse for giving the ATUPS grant allowing the collaboration with the Wolfson Atmospheric Chemistry Laboratories of York in the research group of Mathew J. Evans.

## 880 References

- Amos, H. M., Jacob, D. J., Holmes, C. D., Fisher, J. A., Wang, Q., and co authors: Gas-particle partitioning of atmospheric Hg(II) and its effect on global mercury deposition, *Atmospheric Chemistry and Physics*, 12, 591–603, 2012.
- Aumont, B.: *Modélisation de la chimie troposphérique*, Val de Marne, 2005.
- 885 Banerjee, A., Archibald, A. T., Maycock, A. C., Telford, P., Abraham, N. L., and co authors: Lightning NO<sub>x</sub>, a key chemistry-climate interaction: impacts of future climate change and consequences for tropospheric oxidising capacity, *Atmospheric Chemistry and Physics*, 14, 9871–9881, 2014.
- Bechtold, P., Bazile, E., Guichard, F., Mascart, P., and Richard, E.: A mass-flux convection scheme for regional and global models, *Q. J. R. Meteorol. Soc.*, 127, 869–886, 2000.
- 890 Bey, I., Jacob, D. J., Yantosca, R. M., Logan, J. A., Field, B. D., Fiore, A. M., Li, Q., Liu, H. Y., Mickley, L. J., and Schultz, M. G.: Global modeling of tropospheric chemistry with assimilated meteorology: model description and evaluation, *Journal of Geophysical Research*, 106, 23,073–23,095, 2001.
- Bian, H. and Prather, M. J.: Fast-J2: Accurate simulation of stratospheric photolysis in global chemical models, *Journal of Atmospheric Chemistry*, 41, 281–296, 2002.
- 895 Cariolle, D., Caro, D., Paoli, R., Hauglustaine, D. A., Cuénot, B., Cozic, A., and Paugam, R.: Parametrization of plume chemistry into large-scale atmospheric models: application to aircraft NO<sub>x</sub> emissions, *Journal of Geophysical Research*, 114, 2009.
- Choi, Y., Kim, J., Eldering, A., Osterman, G., Yung, Y. L., Gu, Y., and Liou, K. N.: Lightning and anthropogenic NO<sub>x</sub> sources over the United States and the western North Atlantic Ocean: impact on OLR and radiative effects, *Geophysical Research Letters*, 36, 2009.
- 900 Christian, H. J., Blakeslee, R. J., Boccippio, D. J., Boeck, W. L., and et al., D. E. B.: Global frequency and distribution of lightning as observed from space by the Optical Transient Detector, *Journal of Geophysical Research*, 108, 4005, 2003.
- Cohard, J.-M. and Pinty, J. P.: A comprehensive two-moment warm microphysical bulk scheme. I: Description and tests, *Q. J. R. Meteorol. Soc.*, 126, 1815–1842, 2000.
- 905 Cooper, M., Martin, R. V., Wespes, C., Coheur, P.-F., Clerbaux, C., and co authors: Tropospheric nitric acid columns from the IASI satellite instrument interpreted with a chemical transport model: implications for parameterizations of nitric oxide production by lightning, *Journal of Geophysical Research*, 119, 10,068–10,079, 2014.
- 910 Cuxart, J., Bougeault, P., and Redelsperger, J. L.: A turbulence scheme allowing for mesoscale and large-eddy simulations, *Q. J. R. Meteorol. Soc.*, 126, 1–30, 1999.
- Damian, V., Sandu, A., Damian, M., Potra, F., and Camichael, G. R.: The kinetic preprocessor KPP - a software environment for solving chemical kinetics, *Computers and Chemical Engineering*, 26, 1567–1579, 2002.
- Dye, J. E., Ridley, B. A., Skamarock, W., Barth, M., and Venticinque, M.: An overview of the Stratospheric-Tropospheric experiment: radiation, aerosols, and ozone (STERAO)-Deep convection experiment with results for the July 10, 1996 storm, *Journal of Geophysical Research*, 105, 10,023–10,045, 2000.
- 915 Emmerson, K. M. and Evans, M. J.: Comparison of tropospheric gas-phase chemistry schemes for use within global models, *Atmospheric Chemistry and Physics*, 9, 1831–1845, 2009.

Evans, M. J. and Jacob, D. J.: Impact of new laboratory studies of N<sub>2</sub>O<sub>5</sub> hydrolysis on global model budgets of tropospheric nitrogen oxides, ozone, and OH, *Geophysical Research Letters*, 32, 2005.

Franzblau, E.: Electrical discharges involving the formation of NO, NO<sub>2</sub>, HNO<sub>3</sub> and O<sub>3</sub>, *Journal of Geophysical Research*, 96, 22,337–22,345, 1991.

Gregory, D., Morcrette, J.-J., C., J., Beljaars, A. C. M., and Stockdale, T.: Revision of convection, radiation and cloud schemes in the ECMWF Integrated Forecasting System, *Q. J. R. Meteorol. Soc.*, 126, 1685–1710, 2000.

Grewe, V.: Impact of climate variability on tropospheric ozone, *Science of the Total Environment*, 374, 167–181, 2007.

Guenther, A. B., Jiang, X., Heald, C. L., Sakulyanontvittaya, T., and D, T.: The model of emissions of gases and aerosols from nature version 2.1 (MEGAN2.1): an extended and updated framework for modeling biogenic emissions, *Geoscientific Model Development*, 5, 1471–1492, 2012.

Hauglustaine, D., Emmons, L., Newchurch, M., Brasseur, G., Takao, T., Matsubara, K., Johnson, J., Ridley, B., Stith, J., and Dye, J.: On the role of lightning NO<sub>x</sub> in the formation of tropospheric ozone plumes: a global model perspective, *Journal of Atmospheric Chemistry*, 38, 277–294, 2001.

Hauglustaine, D. A., Granier, C., and Brasseur, G. P.: Impact of present aircraft emissions of nitrogen oxides on tropospheric ozone and climate forcing, *Geophysical Research Letters*, 21, 2031–2034, 1994.

Hudman, R. C., Jacob, D. J., Turquety, S., Leibensperger, E. M., Murray, L. T., and al.: Surface and lightning sources of nitrogen oxides over the United States: Magnitudes, chemical evolution, and outflow, *Journal of Geophysical Research*, 112, 2007.

Huntrieser, H., Schlager, H., Feigl, C., and Höller, H.: Transport and production of NO<sub>x</sub> in electrified thunderstorms: survey of previous studies and new observations at midlatitudes, *Journal of Geophysical Research*, 103, 28,247–28,264, 1998.

Huntrieser, H., Feigl, C., Schlager, H., Schröder, F., Gerbig, C., and van Velthoven, P.: Airborne measurements of NO<sub>x</sub>, tracer species, and small particles during the European Lightning Nitrogen Oxides Experiment, *Journal of Geophysical Research*, 107, 4113, 2002.

Huszar, P., Cariolle, D., Paoli, R., Halenka, T., Belda, M., and al.: Modeling the regional impact of ship emissions on NO<sub>x</sub> and ozone levels over the Eastern Atlantic and Western Europe using ship plume parameterization, *Atmospheric Chemistry and Physics*, 10, 6645–6660, 2010.

Jacobson, M. Z. and Turco, R. P.: SMVGEAR: a sparse-matrix, vectorized gear code for atmospheric models, *Atmospheric Environment*, 28, 273–284, 1994.

Jaéglé, L., Jacob, D. J., Wang, Y., Weinheimer, A. J., Ridley, B. A., and co authors: Sources and chemistry of NO<sub>x</sub> in the upper troposphere over the United States, *Geophysical Research Letters*, 25, 1705–1708, 1998.

Jenkin, M. E., Saunders, S. M., and Pilling, M. J.: The tropospheric degradation of volatile organic compounds: a protocol for mechanism development, *Atmospheric Environment*, 31, 81–104, 1997.

Klemp, J. B. and Wilhelmson, R. B.: The simulation of three-dimensional convective storm dynamics, *Journal of Atmospheric Sciences*, 35, 1070–1096, 1978.

Knollenberg, R. G.: Measurements of the growth of the ice budget in a persisting contrail, *Journal of the Atmospheric Sciences*, 29, 1367–1374, 1972.

- Knollenberg, R. G., Kelly, K., and Wilson, J. C.: Measurements of high number densities of ice crystals in the tops of tropical cumulonimbus, *Journal of Geophysical Research*, 98, 8639–8664, 1993.
- 960 Labrador, L. J., von Kuhlmann, R., and Lawrence, M. G.: Strong sensitivity of the global mean OH concentration and the tropospheric oxidizing efficiency to the source of NO<sub>x</sub> from lightning, *Geophysical Research Letters*, 31, 2004.
- Lafore, J. P., Stein, J., Asencio, N., Bougeault, P., Ducrocq, V., Duron, J., Fischer, C., Hérel, P., Mascart, P., Masson, V., Pinty, J. P., Redelsperger, J. L., Richard, E., and de Arellano, J. V.-G.: The meso-NH Atmospheric
- 965 Simulation System. Part I: adiabatic formulation and control simulations, *Ann. Geophysicae*, 16, 90–109, 1998.
- Lange, L., Hoor, P., Helas, G., Fischer, H., and et al., D. B.: Detection of lightning-produced NO in the mid-latitude upper troposphere during STREAM 1998, *Journal of Geophysical Research*, 106, 27,777–27,785, 2001.
- 970 Lascaux, F., Richard, E., and Pinty, J. P.: Numerical simulations of three different MAP IOPs and the associated microphysical processes, *Q. J. R. Meteorol. Soc.*, 132, 1907–1926, 2006.
- Lin, J.-T. and McElroy, M. B.: Impacts of boundary layer mixing on pollutant vertical profiles in the lower troposphere: implications to satellite remote sensing, *Atmospheric Environment*, 44, 1726–1739, 2010.
- Lin, S.-J. and Rood, R. B.: Multidimensional flux-form semi-lagrangian transport scheme, *Monthly Weather*
- 975 Review, 124, 2046–2070, 1996.
- Lin, X., Trainer, M., and Liu, S. C.: On the nonlinearity of the tropospheric ozone production, *Journal of Geophysical Research*, 93, 15 879–15 888, 1988.
- Liu, H., Jacob, D. J., Rey, I., and Yantosca, R. M.: Constraints from <sup>210</sup>Pb and <sup>7</sup>Be on wet deposition and transport in a global three-dimensional chemical tracer model driven by assimilated meteorological fields,
- 980 *Journal of Geophysical Research*, 106, 12,109–12,128, 2001.
- Lobert, J. M., Keene, W. C., Logan, J. A., and Yevich, R.: Global chlorine emissions from biomass burning: reactive chlorine emissions inventory, *Journal of Geophysical Research*, 104, 8373–8389, 1999.
- Madronich, S. and Flocke, S.: *Environmental Photochemistry*, Springer, 1999.
- Martin, R. V., Jacob, D. J., Logan, J. A., Bey, I., Yantosca, R. M., Staudt, A. C., Li, Q., Fiore, A. M., Duncan,
- 985 B. N., and Liu, H.: Interpretation of TOMS observations of tropical tropospheric ozone with a global model and in situ observations, *Journal of Geophysical Research*, 107, 4351, 2002.
- Martin, R. V., Sauvage, B., Folkins, I., Sioris, C. E., Boone, C., Bernath, P., and Ziemke, J.: Space-based constraints on the production of nitric oxide by lightning, *Journal of Geophysical Research*, 112, 2007.
- Monks, P. S.: Gas-phase radical chemistry in the troposphere, *Chemical Society Reviews*, 34, 376–395, 2005.
- 990 Moorthi, S. and Suarez, M. J.: Relaxed Arakawa-Schubert: a parameterization of moist convection for general circulation models, *Monthly Weather Review*, 120, 978–1002, 1991.
- Murray, L. T., Jacob, D. J., Logan, J. A., Hudman, R. C., and Koshak, J.: Optimized regional and interannual variability of lightning in a global chemical transport model constrained by LIS/OTD satellite data, *Journal of Geophysical Research*, 117, 2012.
- 995 Olivier, J. G. J.: Recent trends in global greenhouse gas emissions: regional trends and spatial distribution of key sources, *Environment Sciences*, 2, 81–89, 2005.

- Ott, L. E., Pickering, K. E., Stenchikov, G. L., Allen, D. J., DeCaria, A. J., and co authors: Production of lightning NO<sub>x</sub> and its vertical distribution calculated from three-dimensional cloud-scale chemical transport model simulations, *Journal of Geophysical Research*, 115, 2010.
- 1000 Paoli, R., Cariolle, D., and Sausen, R.: Review of effective emissions modeling and computation, *Geoscientific Model Development*, 4, 643–667, 2011.
- Pickering, K. E., Thompson, A. M., Dickerson, R. R., Luke, W. T., MacNamara, D. P., Greenberg, J. P., and Zimmerman, P. R.: Model calculations of tropospheric ozone production potential following observed convective events, *Journal of Geophysical Research*, 95, 14,049–14,062, 1990.
- 1005 Pickering, K. E., and W-K. Tao, Y. W., Price, C., and Müller, J.-F.: Vertical distributions of lightning NO<sub>x</sub> for use in regional and global chemical transport models, *Journal of Geophysical Research*, 103, 31,203–31,216, 1998.
- Pinty, J. P. and Jabouille, P.: A mixed-phase cloud parameterization for use in a mesoscale non-hydrostatic model: simulations of a squall line and of orographic precipitation, *American Meteorological Society*, pp. 217–220, 1999.
- 1010 Price, C. and Rind, D.: A simple lightning parameterization for calculating global lightning distributions, *Journal of Geophysical Research*, 97, 9919–9933, 1992.
- Price, C. and Rind, D.: Possible implications of global climate change on global lightning distributions and frequencies, *Journal of Geophysical Research*, 99, 10,823–10,831, 1994.
- 1015 Sander, S. P., Friedl, R. R., Golden, D. M., Kurylo, M. J. M., and et al., G. K. M.: Chemical kinetics and photochemical data for use in atmospheric studies, evaluation number 15, Tech. rep., NASA, 2006.
- Saunders, S. M., Jenkin, M. E., Derwent, R. G., and Pilling, M. J.: Protocol for the development of the Master Chemical Mechanism, MCM v3 (Part A): tropospheric degradation of non-aromatic volatile organic compounds, *Atmospheric Chemistry and Physics*, 3, 161–180, 2003.
- 1020 Sauvage, B., Martin, R. V., van Donkelaar, A., and Ziemke, J. R.: Quantification of the factors controlling tropical tropospheric ozone and the South Atlantic maximum, *Journal of Geophysical Research*, 112, 2007a.
- Sauvage, B., Martin, R. V., van Donkelaar, A., Liu, X., Chance, K., Jaeglé, L., Palmer, P. I., Wu, S., and Fu, T. M.: Remote sensed and in situ constraints on processes affecting tropical tropospheric ozone, *Atmospheric Chemistry and Physics*, 7, 815–838, 2007b.
- 1025 Schumann, U. and Huntrieser, H.: The global lightning-induced nitrogen oxides source, *Atmospheric Chemistry and Physics*, 7, 3823–3907, 2007.
- Stark, M. S., Harrison, J. T. H., and Anastasi, C.: Formation of nitrogen oxides by electrical discharges and implications for atmospheric lightning, *Journal of Geophysical Research*, 101, 6963–6969, 1996.
- Stith, J., Dye, J., Ridley, B., Laroche, P., Defer, E., Hübler, G., Zerr, R., and Venticinque, M.: NO signatures from lightning flashes, *Journal of Geophysical Research*, 104, 16,081–16,089, 1999.
- 1030 Stockwell, D. Z., Giannakopoulos, C., Plantevin, P. H., Carver, G. D., Chipperfield, M. P., Law, K. S., Pyle, J. A., Shallcross, D. E., and Wang, K. Y.: Modelling NO<sub>x</sub> from lightning and its impact on global chemical fields, *Atmospheric Environment*, 33, 4477–4493, 1999.
- Streets, D. G., Zhang, Q., Wang, L., He, K., Hao, J., and al.: Revisiting China's CO emissions after the Transport and Chemical evolution over the Pacific (TRACE-P) mission: Synthesis of inventories, atmospheric modeling, and observations, *Journal of Geophysical Research*, 111, 2006.
- 1035



- Teyss  dre, H., Michou, M., Clark, H. L., Josse, B., Karcher, F., Olivi  , D., Peuch, V.-H., Saint-Martin, D., Cariolle, D., Atti  , J.-L., N  d  lec, P., Ricaud, P., Thouret, V., van der A, R. J., Volz-Thomas, A., and Cheroux, F.: A new tropospheric and stratospheric chemistry and transport model MOCAGE-Climat for multi-year studies: evaluation of the present-day climatology and sensitivity to surface processes, *Atmospheric Chemistry and Physics*, 7, 5815–5860, 2007.
- 1040 Tost, H., J  ckel, P., and Lelieveld, J.: Lightning and convection parameterisations - uncertainties in global modelling, *Atmospheric Chemistry and Physics*, 7, 4553–4568, 2007.
- Trier, S. B. and Sharman, R. D.: Convection-permitting simulations of the environment supporting widespread
- 1045 turbulence within the upper-level outflow of a mesoscale convective system, *American Meteorological Society*, 137, 1972–1990, 2008.
- Tulet, P., Crassier, V., Solmon, F., Guedalia, D., and Rosset, R.: Description of the Mesoscale Nonhydrostatic chemistry model and application to a transboundary pollution episode between northern France and southern England, *Journal of Geophysical Research*, 108, 4021, 2003.
- 1050 Tulet, P., Grini, A., Griffin, R. J., and Petitcol, S.: ORILAM-SOA: A computationally efficient model for predicting secondary organic aerosols in three-dimensional atmospheric models, *Journal of Geophysical Research*, 111, 2006.
- van der Werf, G. R., Randerson, J. T., Giglio, L., G. J. Collatz, M. M., Kasibhatla, P. S., Morton, D. C., DeFries, R. S., Jin, Y., and van Leeuwen, T. T.: Global fire emissions and the contribution of deforestation, savanna, forest, agricultural, and peat fires (1997-2009), *Atmospheric Chemistry and Physics*, 10, 11 707–11 735,
- 1055 2010.
- Wang, Q., Jacob, D. J., Fisher, J. A., Mao, J., Leibensperger, E. M., and co authors: Sources of carbonaceous aerosols and deposited black carbon in the Arctic in winter-spring: implications for radiative forcing, *Atmospheric Chemistry and Physics*, 11, 12 453–12 473, 2011.
- 1060 Wang, Y., Jacob, D. J., and Logan, J. A.: Global simulation of tropospheric O<sub>3</sub>-NO<sub>x</sub>-hydrocarbon chemistry - 1. Model formulation, *Journal of Geophysical Research*, 103, 10,713–10,725, 1998.
- Weiss, S. A., MacGorman, D. R., and Calhoun, K. M.: Lightning in the anvils of supercell thunderstorms, *Monthly Weather Review*, 140, 2064–2079, 2012.
- Wennberg, P. O., Hanisco, T. F., Jaegl  , L., Jacob, D. J., Hinst, E. J., Lanzendorf, E. J., Anderson, J. G.,
- 1065 Gao, R. S., and al.: Hydrogen radicals, nitrogen radicals and the production of O<sub>3</sub> in the upper troposphere, *Science*, 279, 1998.
- Wesely, M. L.: Parameterization of surface resistances to gaseous dry deposition in regional-scale numerical models, *Atmospheric Environment*, 23, 1293–1304, 1989.
- WMO: Scientific Assessment of Ozone Depletion: 1998, Tech. rep., World Meteorological Organization, 1999.
- 1070 Yevich, R. and Logan, J. A.: An assessment of biofuel use and burning of agricultural waste in the developing world, *Global Biogeochemical Cycles*, 17, 1095, 2003.
- Yienger, J. J. and Levy, H.: Empirical model of global soil-biogenic NO<sub>x</sub> emissions, *Journal of Geophysical Research*, 100, 11,447–11,464, 1995.
- Zhang, Q., Streets, D. G., G. R. Carmichael, K. B. H., Huo, H., and al.: Asian emissions in 2006 for the NASA
- 1075 INTEx-B mission, *Atmospheric Chemistry and Physics*, 9, 5131–5153, 2009.

Zhang, R., Tie, X., and Bond, D. W.: Impacts of anthropogenic and natural NO<sub>x</sub> sources over the U.S. on tropospheric chemistry, *Proceedings of the National Academy of Sciences of the United States of America*, 100, 1505–1509, 2003.

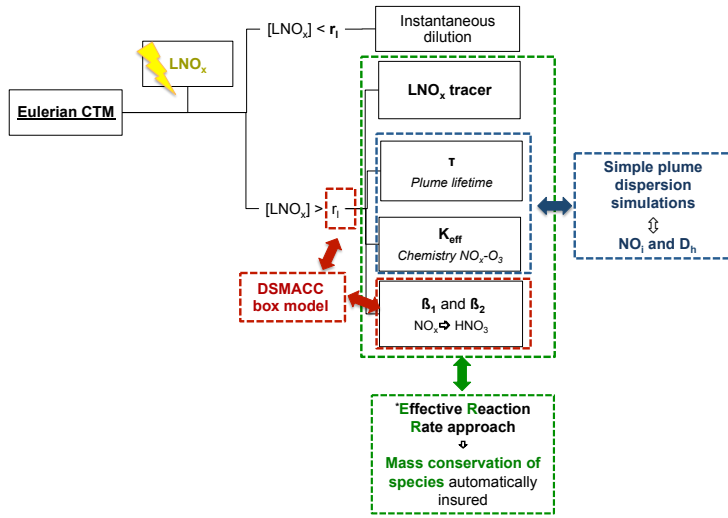


**Figure 1.** The Diagram of the lightning  $\text{NO}_x$  plume parameterization based on the Effective Reaction Rate approach. The arrows link the parameters to their estimate approach. The red boxes are for the parameters estimated with the DSMACC model and the blue boxes are related to the parameters calculated with the simple plume dispersion model. Finally the green boxes show the Effective Reaction Rate approach in the GEOS-Chem CTM.

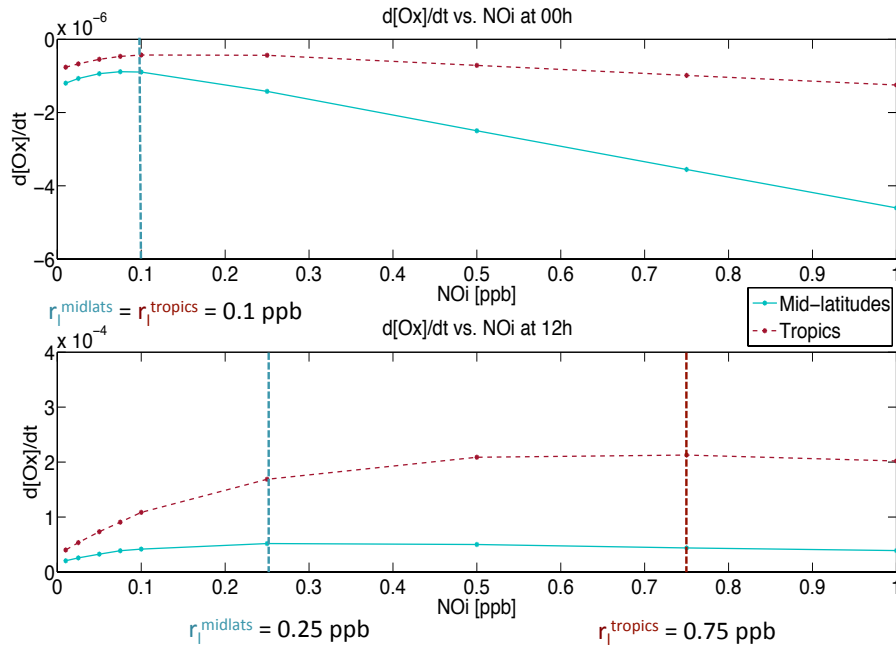


**Figure 2.**  $r_l$  critical value and odd oxygen trends from DSMACC chemistry box model simulations for mid-latitudes (solid line) and tropics (dotted line) (a) at midnight (upper panel) and (b) at midday (bottom panel).

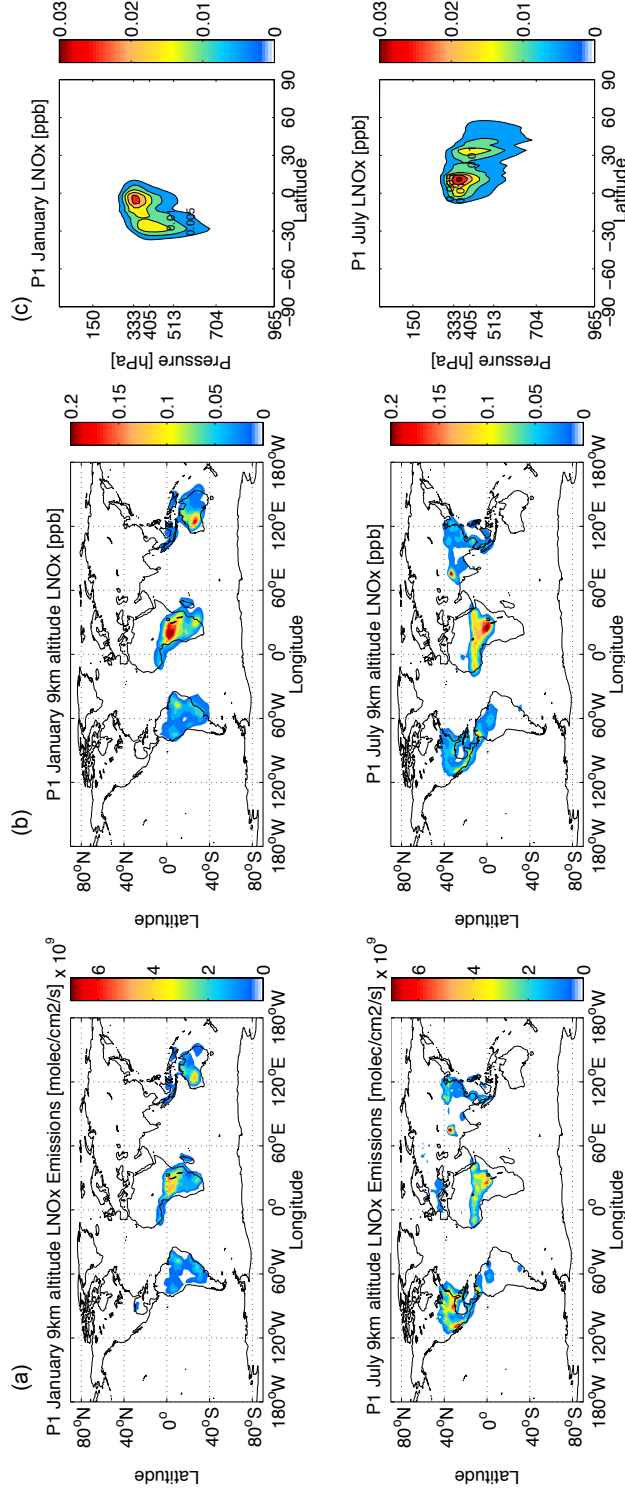


**Figure 3.** (left panels, a) Geographical distributions at 9 km altitude of lightning  $NO_x$  emissions, (middle panels, b) the geographical distributions of the related  $LNO_x$  tracer (in ppb) and (right panels, c) the zonal averaged of the  $LNO_x$  tracer (in ppb), for January (top) and July (bottom). Experiment  $P1$ , using  $\tau$  and  $K_{eff}$  determined with  $D_h = 15 \text{ m}^2 \cdot \text{s}^{-1}$  and  $NO_i^{mean}$ , performed with the GEOS-Chem model.

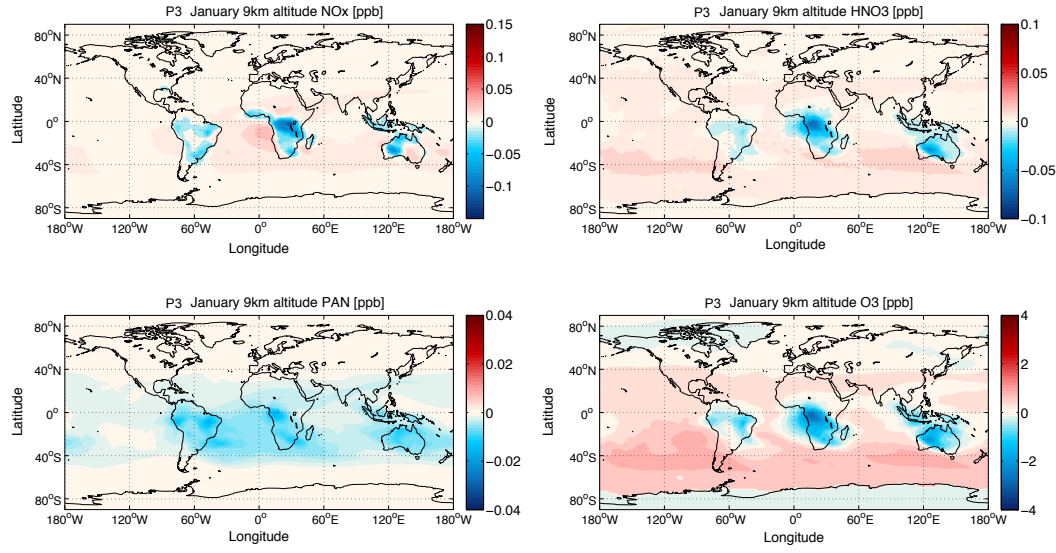


**Figure 4.** Geographical distributions of  $NO_x$ ,  $HNO_3$ , PAN, and  $O_3$  variations (in ppb) at 9 km altitude for January from the absolute difference ( $P3$ ) between  $P1$  and BC experiments.  $P1$  was performed using  $\tau$  and  $K_{eff}$  determined with  $D_h = 15 \text{ m}^2 \cdot \text{s}^{-1}$  and  $NO_i^{mean}$  with GEOS-Chem.

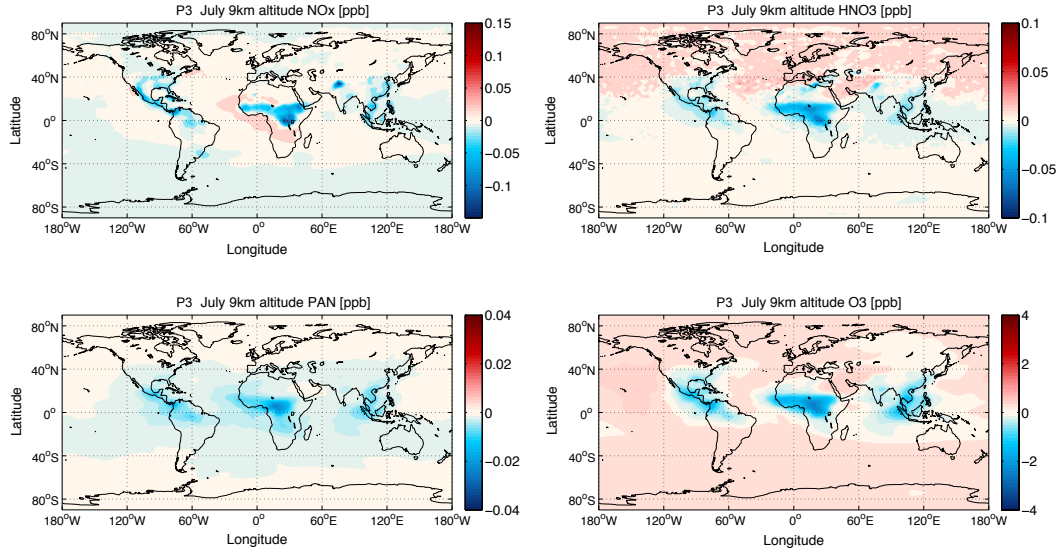


**Figure 5.** Geographical distributions of  $NO_x$ ,  $HNO_3$ , PAN, and  $O_3$  variations (in ppb) at 9 km altitude for July from the absolute difference ( $P3$ ) between  $P1$  and BC experiments.  $P1$  was performed using  $\tau$  and  $K_{eff}$  determined with  $D_h = 15 \text{ m}^2 \cdot \text{s}^{-1}$  and  $NO_i^{mean}$  with GEOS-Chem.

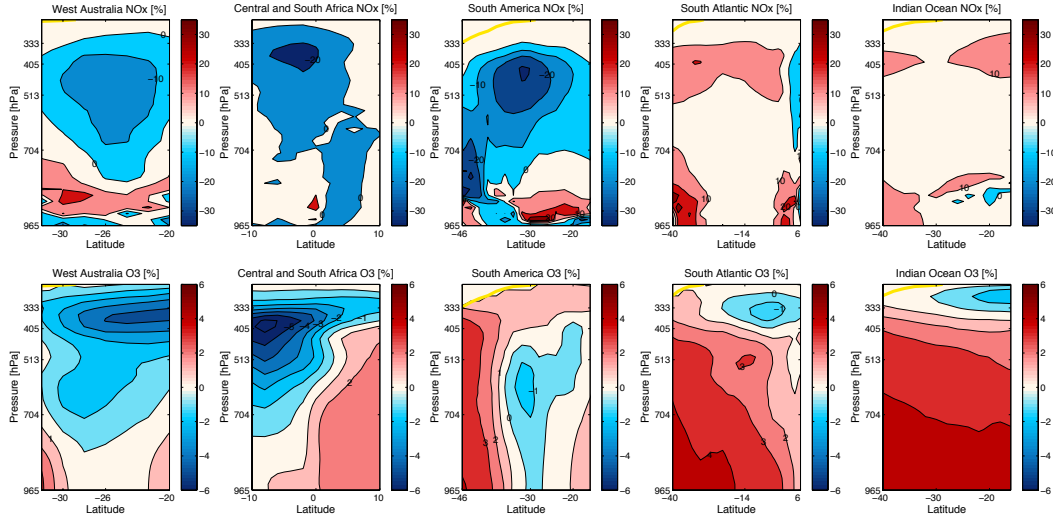


**Figure 6.** Zonal averaged  $NO_x$  (upper panels) and  $O_3$  (bottom panels) variations (in %) over the regions characterized by strong  $NO_x$  emissions for January (the yellow solid line represents the tropopause level), from the relative difference between  $P1$  and  $BC$  experiments ( $(P1-BC)/BC$ ).  $P1$  was performed using  $\tau$  and  $K_{eff}$  determined with  $D_h = 15 \text{ m}^2 \cdot \text{s}^{-1}$  and  $NO_i^{mean}$  with GEOS-Chem.

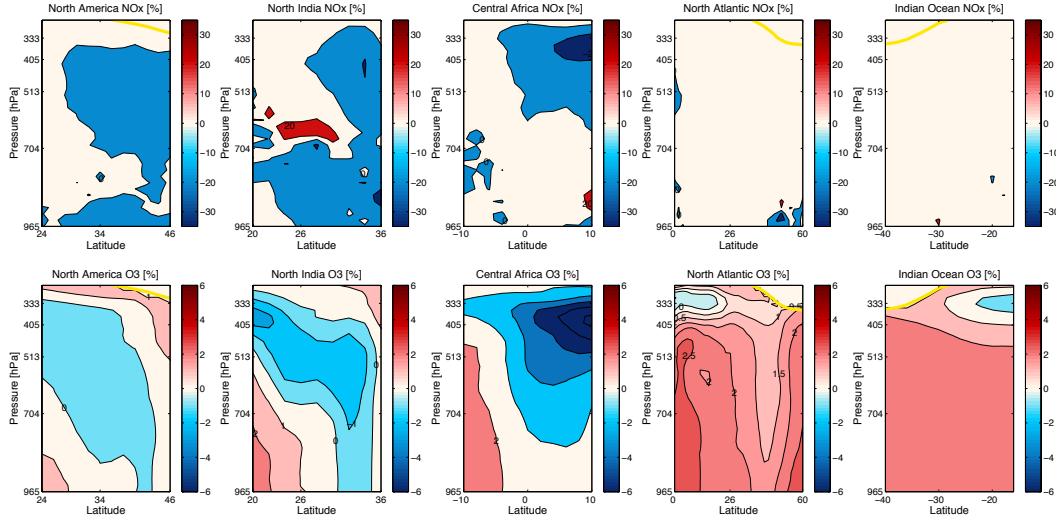


**Figure 7.** Zonal averaged  $NO_x$  (upper panels) and  $O_3$  (bottom panels) variations (in %) over the regions characterized by strong  $NO_x$  emissions for July (the yellow solid line represents the tropopause level), from the relative difference between  $P1$  and  $BC$  experiments ( $(P1-BC)/BC$ ).  $P1$  was performed using  $\tau$  and  $K_{eff}$  determined with  $D_h = 15 \text{ m}^2 \cdot \text{s}^{-1}$  and  $NO_i^{mean}$  with GEOS-Chem.

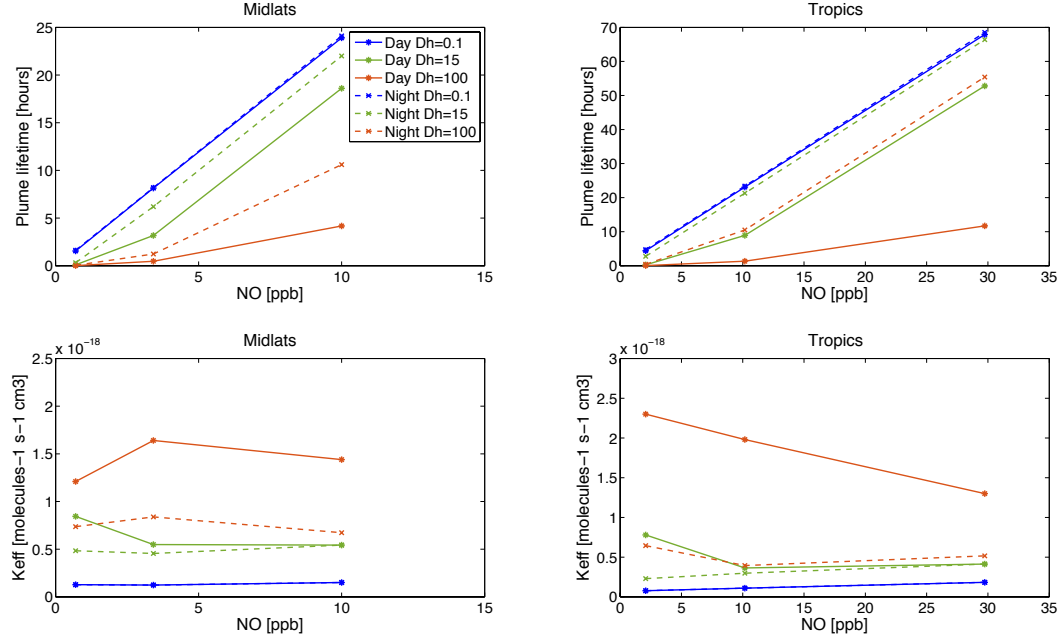


**Figure 8.** The plume lifetime ( $\tau$ , upper panels) and the effective reaction rate constant ( $K_{eff}$ , bottom panels) depending (i) on the horizontal coefficient diffusion ( $D_h$ , m<sup>2</sup> · s<sup>-1</sup>) for the mid-latitudes (left panels) and the tropics (right panels) and (ii) on the  $NO$  mixing ratio injected by lightning ( $NO_i$ , in ppb).

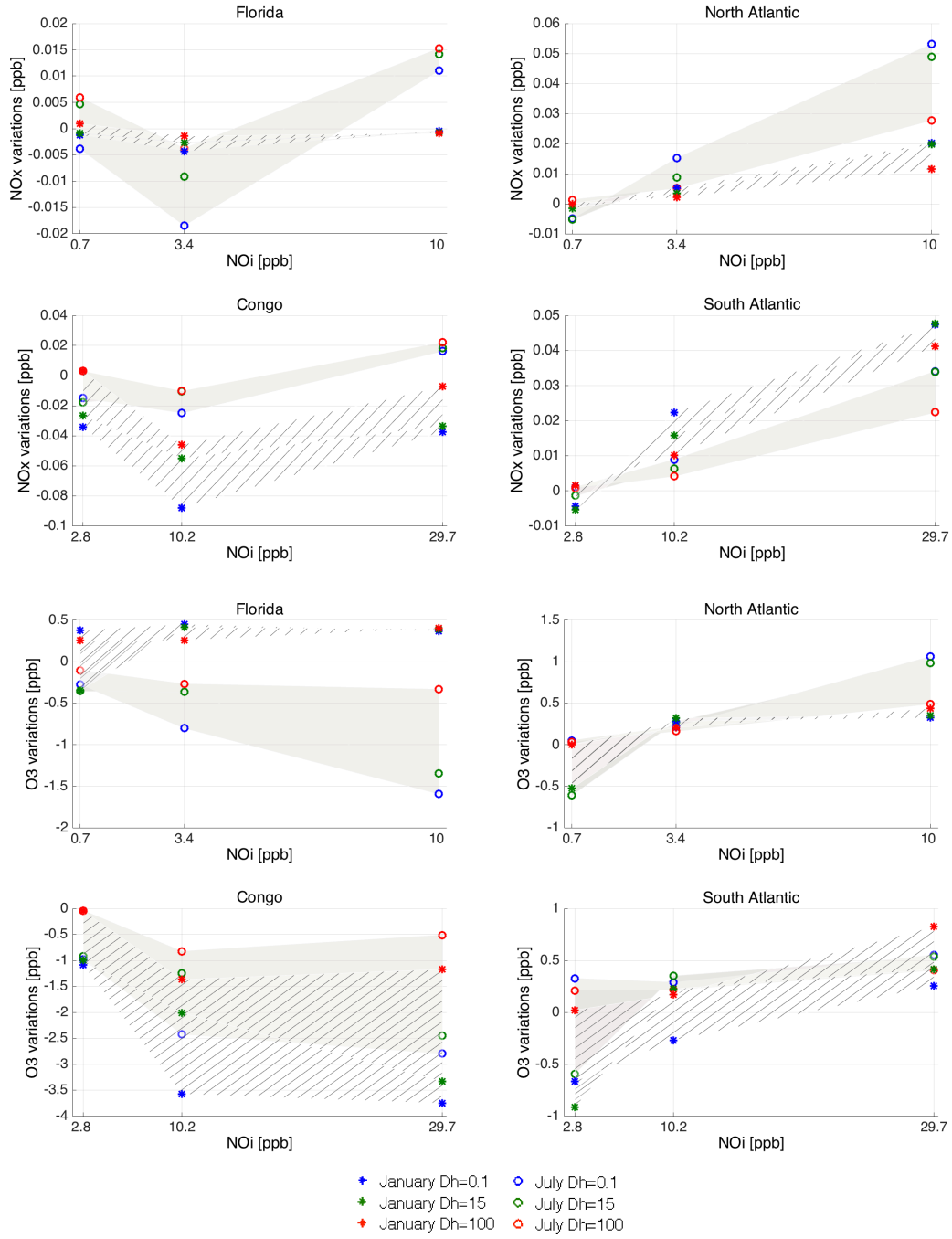


**Figure 9.** The  $NO_x$  (a) and  $O_3$  (b) variability-sensitivity at 9 km altitude depending on the horizontal coefficient diffusion ( $D_h$ ,  $m^2 \cdot s^{-1}$ ) and on the NO mixing ratio injected by lightning ( $NO_i$ , ppb) for the mid-latitudes (Florida and North Atlantic) and the tropics (Congo and South Atlantic). Intervals are hatched in January and non-hatched-filled in grey in July. Markers correspond to the  $NO_x$  variations simulated for  $D_h = 0.1 m^2 \cdot s^{-1}$  (red ones),  $D_h = 15 m^2 \cdot s^{-1}$  (blue ones) and  $D_h = 100 m^2 \cdot s^{-1}$  (green ones).



	TEMP	PRESS	$O_3$	$NO$	$NO_2$	$HNO_3$	$HNO_4$	PAN	$N_2O_5$	CO
Units	(K)	(hPa)	(ppb)	(ppb)	(ppb)	(ppb)	(ppb)	(ppb)	(ppt)	(ppb)
<b>Mid-latitudes</b>	228	313	67	0.04	0.01	0.15	0.02	0.1	2	94
<b>Tropics</b>	240	313	26	0.03	0.003	0.02	0.006	0.03	2.3	93

	$OH$	$HO_2$	$H_2O_2$	$CH_2O$	$CH_4O_2$	$C_3H_8$	$C_5H_8$	$C_2H_4O$	$C_3H_6O$
Units	(ppb)	(ppt)	(ppt)	(ppb)	(ppb)	(ppb)	(ppb)	(ppb)	(ppb)
<b>Mid-latitudes</b>	0.2	4	0.4	0.06	0.1	0.47	0	7.5	4
<b>Tropics</b>	0.06	6	0.34	0.03	0.17	0.13	7.5	7.5	4

**Table 1.** The initial atmospheric parameters and background concentrations of chemical species from GEOS-Chem outputs for the DSMACC chemical box model simulations.

<b>Day</b>						
$\tau$ (hours)	<b>Mid-latitudes</b>			<b>Tropics</b>		
$NO_i$ (ppb)	0.7	3.4	10	2.8	10	29.7
$D_h = 0.1$ ( $m^2 \cdot s^{-1}$ )	1.55	8.14	23.9	4.40	23.1	67.9
$D_h = 15$ ( $m^2 \cdot s^{-1}$ )	0.1	3.17	18.6	0.27	8.90	52.8
$D_h = 100$ ( $m^2 \cdot s^{-1}$ )	0.01	0.47	4.17	0.04	1.32	11.7
<b>Night</b>						
$\tau$ (hours)	<b>Mid-latitudes</b>			<b>Tropics</b>		
$NO_i$ (ppb)	0.7	3.4	10	2.8	10	29.7
$D_h = 0.1$ ( $m^2 \cdot s^{-1}$ )	1.62	8.19	24.1	4.74	23.4	68.5
$D_h = 15$ ( $m^2 \cdot s^{-1}$ )	0.31	6.19	22	2.77	21.3	66.4
$D_h = 100$ ( $m^2 \cdot s^{-1}$ )	0.05	1.23	10.6	0.43	10.5	55.4

**Table 2.** The plume lifetime  $\tau$  (hours) calculated for mid-latitudes and tropics depending on the initial  $NO$  mixing ratio injected by lightning emissions ( $NO_i$ , ppb) and the horizontal diffusion coefficient ( $D_h$ ,  $m^2 \cdot s^{-1}$ ) for day (upper table) and night conditions (bottom table).

<b>Day</b>						
$K_{eff}(10^{-19} \text{ molecules}^{-1} \cdot \text{s}^{-1} \cdot \text{cm}^3)$	<b>Mid-latitudes</b>			<b>Tropics</b>		
$NO_i \text{ (ppb)}$	0.7	3.4	10	2.8	10	29.7
$D_h = 0.1 \text{ (m}^2 \cdot \text{s}^{-1}\text{)}$	1.28	1.24	1.51	0.77	1.2	1.83
$D_h = 15 \text{ (m}^2 \cdot \text{s}^{-1}\text{)}$	8.44	5.49	5.43	7.79	3.64	4.13
$D_h = 100 \text{ (m}^2 \cdot \text{s}^{-1}\text{)}$	12.1	16.4	14.4	23	19.8	13
<b>Night</b>						
$K_{eff}(10^{-19} \text{ molecules}^{-1} \cdot \text{s}^{-1} \cdot \text{cm}^3)$	<b>Mid-latitudes</b>			<b>Tropics</b>		
$NO_i \text{ (ppb)}$	0.7	3.4	10	2.8	10	29.7
$D_h = 0.1 \text{ (m}^2 \cdot \text{s}^{-1}\text{)}$	1.28	1.24	1.51	0.77	1.10	1.83
$D_h = 15 \text{ (m}^2 \cdot \text{s}^{-1}\text{)}$	4.84	4.55	5.43	2.3	2.98	4.13
$D_h = 100 \text{ (m}^2 \cdot \text{s}^{-1}\text{)}$	7.36	8.39	6.73	6.45	3.94	5.16

**Table 3.** The effective reaction rate constant  $K_{eff}$  ( $10^{-19} \text{ molecules}^{-1} \cdot \text{s}^{-1} \cdot \text{cm}^3$ ) in mid-latitudes and tropics depending on the initial  $NO$  mixing ratio injected by lightning emissions ( $NO_i$ , ppb) and the horizontal diffusion coefficient ( $D_h$ ,  $\text{m}^2 \cdot \text{s}^{-1}$ ) for day (upper table) and night conditions (bottom table).

<b>Day</b>						
$\beta_1$ ( $10^{-4}$ )	<b>Mid-latitudes</b>			<b>Tropics</b>		
$NO_i$ (ppb)	0.7	3.4	10	2.8	10	29.7
Aerosols	2.53	3.34	3.45	2.51	2.95	2.6
Ice	0.23	0.3	0.3	0.2	0.23	0.3
Mean	1.38	1.8	1.88	1.34	1.59	1.47
<b>Night</b>						
$\beta_2$ ( $10^{-3}$ )	<b>Mid-latitudes</b>			<b>Tropics</b>		
$NO_i$ (ppb)	0.7	3.4	10	2.8	10	29.7
Aerosols	14.3	9.89	8	4.9	1.69	0.24
Ice	14.4	9.96	8.06	4.89	1.70	0.24
Mean	14.4	9.92	8.03	4.88	1.7	0.24

**Table 4.** The fractions of  $NO_x$  conversion into  $HNO_3$  within the plume ( $\beta_1$  and  $\beta_2$ ) in mid-latitudes and tropics depending on the initial  $NO$  mixing ratio injected by lightning emissions ( $NO_i$ , ppb) and on particles for day (upper table) and night conditions (bottom table).

Parameters				Experiments								
				P1				P2				
$D_h \text{ (} m^2 \cdot s^{-1} \text{)}$	0.1			15			100			15		
$NO_i \text{ (ppb)}$	Min	Mean	Max	Min	Mean	Max	Min	Mean	Max	Mean		
Mid-latitudes	0.7	3.4	10	0.7	3.4	10	0.7	3.4	10	3.4		
Tropics	2.8	10.2	29.7	2.8	10.2	29.7	2.8	10.2	29.7	10.2		
$\beta_1$	Mean						0			$Min$	$Mean$	$Max$
$\beta_2$	Mean						0			$Min$	$Mean$	$Max$

**Table 5.** Values of the parameters for the plume parameterization corresponding to the experiments *P1* and *P2*.

		JANUARY				JULY			
		Mid-latitudes		Tropics		Mid-latitudes		Tropics	
		Florida	North Atlantic	Congo	South Atlantic	Florida	North Atlantic	Congo	South Atlantic
$\Delta NO_x \pm$	$[-1.7; +1.8]$	$[-8.2; +1.7]$	$[-33.1; +29.7]$	$[-6.5; +6.9]$	$[-9.3; +5.4]$	$[-21.1; +6.6]$	$[-14.3; +21]$	$[-11.5; +2.6]$	
$\Delta O_3 \pm$	$[-0.16; +0.72]$	$[-0.12; +0.53]$	$[-1.56; +2.16]$	$[-0.49; +0.94]$	$[-0.44; +1.01]$	$[-0.49; +0.66]$	$[-1.18; +1.93]$	$[-0.14; +0.92]$	

**Table 6.** The ~~variability~~ **sensitivity** of  $NO_x$  (in ppt) and  $O_3$  (in ppb) depending on the horizontal diffusion coefficient ( $D_h, m^2 \cdot s^{-1}$ ) and on the  $NO_i$  mixing ratio (ppb) injected by lightning for mid-latitudes (Florida and North Atlantic) and tropics (Congo and South Atlantic) in January and July.

JANUARY			JULY		
	Mid-latitudes		Tropics		Tropics
	Florida	North Atlantic	Congo	South Atlantic	
$\Delta NO_x \pm \cdot 10^{-2}$	$[-1.6; -0.06]$	$[-2.3; -2.3]$	$[-2.3; +0.9]$	$[+0.3; +0.6]$	$[-0.9; -0.4]$
$\Delta O_3 \pm \cdot 10^{-4}$	$[-9; +5]$	$[-9; +4]$	$[-3; +22]$	$[-10; +11]$	$[-30; -2]$

**Table 7.** The ~~variability~~sensitivity of  $NO_x$  (in ppt) and  $O_3$  (in ppb) depending on  $\beta_1$  and  $\beta_2$  values for mid-latitudes (Florida and North Atlantic) and tropics (Congo and South Atlantic) in January and July. Experiment  $P1$ , using  $D_h = 15 \text{ m}^2 \cdot \text{s}^{-1}$  and  $NO_i^{mean}$ , performed with the GEOS-Chem model.